

# Nanoindentation/scratching at finite temperatures: Insights from atomistic-based modeling

Saeed Zare Chavoshi<sup>1\*</sup>, ShuoZhi Xu<sup>2</sup>

<sup>1</sup>Department of Mechanical Engineering, Imperial College London, London SW7 2AZ, UK

<sup>2</sup>California NanoSystems Institute, University of California, Santa Barbara, Santa Barbara, CA, 93106-6105, USA

\*Corresponding author: *s.zare@imperial.ac.uk*

## Abstract

Atomistic-based multiscale and molecular dynamics modeling are powerful tools to simulate the localized strain problems, offering tremendous opportunities to bridge the knowledge gaps in quantifying and understanding the linkage of plasticity mechanisms and nanomechanical/tribological response of materials at finite temperatures. In this article, we give an overview of these atomistic-based modeling techniques which are amenable to the nanoindentation/scratching at finite temperatures, and briefly describe the pertaining physics, e.g., long range dislocation motion and heat transfer, during nanoindentation/scratching at finite temperatures. We summarize the effects of temperature, loading rate, and crystallographic planes on the process of defect formation and migration as well as the nanomechanical/tribological response of a wide range of crystalline and amorphous materials subject to nanoindentation/scratching. Our review presents unresolved issues and outstanding challenges in atomistic-based modeling of nanoindentation/scratching at finite temperatures and sheds light on the path forward in this emerging research area.

**Keywords:** Atomistic simulation; Multiscale modeling; Finite temperature;  
Nanoindentation/scratching; Nanotribology

## Contents

|  |    |
|--|----|
| 1. Introduction .....                            | 6  |
| 2. Atomistic modeling.....                       | 8  |
| 3. Atomistic-based multiscale modeling.....      | 9  |
| 4. Interatomic potential .....                   | 17 |
| 5. Nanoindentation.....                          | 18 |
| 5.1. Effects of temperature .....                | 18 |
| 5.2. Effects of loading rate .....               | 25 |
| 6. Nanoscratching.....                           | 28 |
| 6.1. Effects of temperature .....                | 28 |
| 6.2. Effects of scratching speed and depth ..... | 32 |
| 6.3. Effects of cutting plane/direction .....    | 34 |
| 7. Summary and outlook .....                     | 35 |
| Acknowledgment.....                              | 40 |
| References.....                                  | 41 |

## Nomenclature

|               |   |
|---------------|---|
| <i>3C-SiC</i> | Cubic silicon carbide   |
| <i>ABOP</i>   | Analytical bond order potential                                     |
| <i>AFEM</i>   | Atomic-based finite element method                                  |
| <i>Al</i>     | Aluminium   |
| <i>Au</i>     | Gold  |
| <i>BCC</i>    | Body-centered cubic   |
| <i>BCM</i>    | Bridging cell method  |
| <i>BMG</i>    | Bulk metallic glass   |
| <i>BMHFT</i>  | Born-Mayer-Huggins-Fumi-Tosi  |
| <i>CAC</i>    | Concurrent atomistic-continuum                                      |
| <i>CADD</i>   | Coupled atomistic/discrete-dislocation                              |
| <i>cBN</i>    | Cubic boron nitride   |
| <i>CLS</i>    | Coupling of length scales   |
| <i>CNT</i>    | Carbon nanotube   |
| <i>CPFEM</i>  | Crystal plasticity finite element method                            |
| <i>Cr</i>     | Chromium  |
| <i>CrN</i>    | Chromium nitride  |
| <i>CTB</i>    | Coherent twin boundary  |
| <i>Cu</i>     | Copper  |
| <i>DAKOTA</i> | Design and analysis kit for optimization and terascale applications |
| <i>DD</i>     | Dislocation dynamics  |
| <i>DDD</i>    | Discrete dislocation dynamics                                       |
| <i>DMD</i>    | Diffusive molecular dynamics  |
| <i>EAM</i>    | Embedded-atom method  |
| <i>EFGM</i>   | Element-free Galerkin method  |
| <i>FCC</i>    | Face-centered cubic   |
| <i>FE</i>     | Finite element  |
| <i>GB</i>     | Grain boundary  |
| <i>GIMP</i>   | Generalized interpolation material point                            |
| <i>GSFE</i>   | Generalized stacking fault energy                                   |
| <i>GULP</i>   | General utility lattice program                                     |

|                        |   |
|------------------------|---|
| <i>HPPT</i>            | High pressure phase transformation            |
| <i>ISE</i>             | Indentation size effect                       |
| <i>L-C</i>             | Lomer-Cottrell                                |
| <i>MC</i>              | Monte Carlo                                   |
| <i>MD</i>              | Molecular dynamics                            |
| <i>MEMS/NEMS</i>       | Micro/Nanoelectromechanical system            |
| <i>MM</i>              | Molecular mechanics                           |
| <i>MMM</i>             | Multiresolution molecular mechanics           |
| <i>MoS<sub>2</sub></i> | Molybdenum disulphide                         |
| <i>MPM</i>             | Material point method                         |
| <i>MS</i>              | Molecular dynamics                            |
| <i>Ni</i>              | Nickel  |
| <i>P-h</i>             | Load-displacement                             |
| <i>POSMat</i>          | Potential optimization software for materials |
| <i>QC</i>              | Quasicontinuum                                |
| <i>REBO</i>            | Reactive empirical bond order                 |
| <i>RKPM</i>            | Reproducing kernel particle method            |
| <i>Si</i>              | Silicon                                       |
| <i>STZ</i>             | Shear transformation zone                     |
| <i>SW</i>              | Stillinger-Weber                              |
| <i>TB-SMA</i>          | Tight-binding-second-moment approximation     |
| <i>TCB</i>             | Temperature-related Cauchy-Born               |
| <i>T<sub>g</sub></i>   | Glass transition temperature                  |
| <i>XRD</i>             | X-ray diffraction                             |
| <i>Zr</i>              | Zirconium                                     |

## 1. Introduction

Indentation is one of the main techniques for probing mechanical properties of engineering materials. Compared with the tension/compression tests, an indentation test is ultra-local and less invasive, in which the indenter is pushed into the surface of the sample. Distinguished by the indentation load  $L$  and the penetration  $h$ , microindentation tests are characterized by  $200 \text{ mN} < L < 2 \text{ N}$  and the  $h > 0.2 \mu\text{m}$ , whereas in nanoindentation  $L$  ranges between a few  $\mu\text{N}$  and about  $200 \text{ mN}$ , while  $h$  varies from a few nm to about a few  $\mu\text{m}$ . Consequently, the indented area in nanoindentation is usually on the nm or a few  $\mu\text{m}$  scale [1, 2]. Another useful technique which can provide extensive insight into the nanoscale mechanical response and plastic deformation of materials is nanoscratching. Unlike nanoindentation, the process of nanoscratching is deviatoric stress-dominative and usually carries a pronounced component of shear, leading to initiation of plasticity mechanisms which may be different from those in nanoindentation [3]. Moreover, while nanoindentation can be used to measure the material hardness, nanoscratching can be employed to evaluate the nanotribological behaviour, frictional, and wear properties of lightly loaded nanostructures, e.g., the thin films and hard coatings utilized in micro/nanoelectromechanical systems (MEMS/NEMS) and other industrial applications [4-6]. As all mechanical and nanotribological properties of materials are temperature-dependent, primarily owing to the increased phonon activities, thermal fluctuation, and phase transformation, small-scale characterization of materials using nanoindentation/scratching at finite temperatures would open up substantial new possibilities in nanomechanics to understand material behaviour at service temperatures and conditions relevant to industrial applications [2, 3]. Material characterization at finite temperatures also provides the opportunity to examine the kinetic aspects of fundamental physics in new materials in new ways.

Experimental studies of nanoindentation/scratching, apart from being expensive, have the

restriction of direct observation of atomic-level events occurring inside the 3D materials on-the-fly within short timespans, i.e., at ps and ns time scales, which are especially important at elevated temperatures. Computational techniques become therefore necessary to capture the essential processes/phenomena during nanoindentation/scratching, most of which are at nm scales where the continuum assumption is known to break down [7]. Take the dislocation modeling in crystalline materials as an example; continuum-based modeling methods like crystal plasticity finite element method (CPFEM) and discrete dislocation dynamics (DDD) are unable to reveal atomistic details such as dislocation core structure and point defect formation/migration which are crucial for understanding physical phenomena in nanoindentation/scratching, such as stacking fault formation, inherent inhomogeneity of plastic deformation, plastic flow localization in shear bands, and the effects of size, geometry, and stress state on yield properties. For these reasons, atomistic simulation methods, such as molecular dynamics (MD), are preferred to understand the deformation mechanisms of materials subjected to nanoindentation/scratching loading.

On the one hand, the nanoindentation/scratching process is highly localized and inherently multiscale, for that (i) the interesting physics is concentrated within a small spatial region, i.e. the localized zone and (ii) outside the localized zone, the material behaviour can be approximated by linear elasticity theory [8, 9]. On the other hand, the time and length scales which can be explored by atomistic simulations are regrettably restricted by computational power. Therefore, atomistic-based multiscale modeling methods are well suited to explore nanoscale properties and behaviour of materials in the localized zone while concurrently simulating far fields using sufficiently large models for the nanoindentation/scratching process.

Some recent review papers [10, 11] have discussed the current state of the art findings and challenges in room (or lower) temperature atomistic and zero temperature multiscale

modeling of nanoindentation, yet, despite its importance, there is no focused review on the emerging area of high temperature nanoindentation/scratching. We are thus motivated to review recent research progress and challenges regarding atomistic simulations of nanoindentation/scratching at high temperatures ( $> 300$  K) as well as atomistic-based multiscale modeling of nanoindentation/scratching at finite temperatures ( $> 0$  K). Pertinent findings on nanotribology at finite temperatures are also highlighted in this article. Future research avenues for atomistic and atomistic-based multiscale modeling of nanoindentation/scratching at finite temperatures, as well as key limitations, are also outlined. We emphasize that this review focuses on atomic-level finite temperature nanoindentation/scratching, hence it will not involve molecular statics (MS), which is a zero temperature modeling technique, DDD and CPFEM, which are continuum-based.

## 2. Atomistic modeling

As an alternative to electronic-structure calculations [12], atomic-level simulation is considered as a powerful tool for studying the microstructure evolution of materials. Atomistic modeling utilizes discrete atomic coordinates as (one of) the indispensable components in simulating material behaviour [13]. There exist several discrete-atom based methods [14-18], including, but not limited to Monte Carlo (MC), MD, and MS. For dynamic problems, kinetic MC and MD are considered as two main families of atomistic simulation techniques. Compared with the kinetic MC method, which probes the configuration space by trial moves of particles, MD integrates Hamilton's equations of motion to move particles to new positions and to let particles obtain new velocities. The MD method is advantageous to MC in that both the configuration space and the phase space are probed, yielding essential information about the dynamical properties of the system. Moreover, the calculation of the heat capacity, compressibility, and interfacial properties can be carried out efficiently and

accurately in MD simulations [19, 20]. Thus, MD is considered as a main practical application of the classical particle dynamics which can be used as an apt bottom-up modeling technique to examine atomic-level events in nanoscale contact problems, e.g., nanoindentation/scratching. MD simulation of nanoindentation/scratching was pioneered by Landman *et al.* [21] and Hoover *et al.* [22] in the early 1990s. Thenceforward, many researchers have considerably contributed to this field and set a foundation for the MD study of the nanoindentation/scratching process.

It is worth noting that one of the main bottlenecks of the classical MD is its short time step, which is typically on the fs scale, arising from the high frequency oscillation of atoms. As a result, a classical MD simulation would take an enormous amount of computation time to adequately capture rare events such as diffusion and dislocation cross-slip. This has motivated the development of various approaches to prevail over the time scale constraints of MD, e.g., the diffusive molecular dynamics (DMD) [23] models that couples diffusional-displacive processes using continuous Gaussian functions to represent atomic density fields [24], and hyperdynamics [25] which uses a modified potential energy function for decreasing energy barriers and speeding up the escape from metastable states without changing the features of the original dynamics. Particularly, DMD [23] and hyperdynamics-based multiscale modeling methods [26, 27] have been applied to high temperature nanoindentation, as will be discussed in Section 5. Interested readers are referred to a recent review by Gerberich and co-workers [28] to comprehend the basics and limitations of these methods.

### 3. Atomistic-based multiscale modeling

As mentioned earlier, classical continuum theories are not appropriate for describing the nanoindentation/scratching process during which the plastic deformation under the indenter involves defect structures, generating a population too small to justify the continuum

assumption. In the meantime, atomistic simulations are limited to relatively small spatial scales. As such, atomistic-based multiscale methodologies, which employ at least one atomistic region, offer a novel approach to cope with these problems by benefiting from the best of both atomistic and continuum techniques, enabling modeling problems that cannot be adequately explored using a full atomistic or continuum simulation. Nevertheless, merging a non-local atomistic model and a usually local continuum model is not trivial [29, 30] and there exist outstanding challenges in avoiding aphysical consequences which may arise from (i) imperfect bonding at the atom-continuum interface, (ii) phonon dynamics and heat transfer at solid-continuum boundaries and (iii) reconstructing atomic positions from a continuum [31]. In terms of materials, some multiscale modeling techniques can only simulate single crystals, in which atomic positions are easily constructed from a continuum, compared with materials with more complex microstructures such as polycrystals. This requirement in constructing atoms from a continuum also implies that most multiscale models cannot be employed to study materials at very high temperatures which may melt and/or become amorphous [32]. A number of reviews [8, 9, 33-39] have appeared in recent years which reflect the technical issues of the multiscale modeling methods. Interested readers are referred to these reviews to extend their knowledge in this field.

While almost all concurrent multiscale models have the capability to handle zero temperature condition, and much success has been achieved in the field of zero temperature multiscale modeling of nanoindentation [40-63], only some of them have dynamic finite temperature formulations. In dynamic setting, because of the large characteristic element size in the continuum region, phonon propagation from the atomic region may not be fully transmitted into the continuum region and may be reflected back. Such spurious phonon reflection gives rise to the temperature gradient and seriously interferes the dynamical equilibrium in the entirely coupled model. Particularly, in the nanoindentation/scratching, the spurious wave

reflection transpires severely, meaning that a large part of the energy imparted by the indenter would be artificially trapped in the atomistic domain, heating it, and destroying the accuracy of the results.

Another major issue in multiscale modeling of nanoindentation/scratching is the long range motion of dislocations, and particularly, the accommodation of dislocations in the continuum and migration of dislocations across the atomistic/continuum domain interface, which are not enabled in most concurrent multiscale methods [64]. Until now, there are only a few concurrent multiscale methods, e.g., the coupled atomistic/discrete-dislocation (CADD) method [65] and the concurrent atomistic-continuum (CAC) method<sup>1</sup> [66-68], which can describe inelastic deformation or plastic flow via the explicit motion of dislocation defects in the continuum region at finite temperatures. Thus, there is scarcity of literature on the robust dynamic multiscale models which can be employed for nanoindentation/scratching at finite temperatures. More importantly, one should keep in mind that although a modicum of advances have been recorded in the literature with regard to the dynamic multiscale modeling formulations, most models are capable of performing dynamic simulations only at relatively low temperatures plausibly due to the wave reflections and thermostats challenges at higher temperatures. In the following, we introduce some multiscale modeling approaches which are of practical relevance and have been adopted to simulate the nanoindentation/scratching process at finite temperatures. We emphasize that most dynamic finite temperature multiscale modeling techniques are still at the stage of method development/validation and have not been used to shed light on new physics of materials [69].

*Atomic-based finite element method (AFEM).* In an AFEM multiscale model of nanoindentation, the substrate is divided into the atomistic, continuum, handshake (linking) regions, and filter layers [70]. A temperature control is imposed in the atomic domain to

---

<sup>1</sup> <http://www.pycac.org/>

dissipate heat while the low-pass filter technique is carried out adjoining the handshaking region. In this way, the dynamical behaviour in terms of the nodal and atomic displacement distribution is achieved and spurious wave reflection at the domain interface is reduced. The AFEM method has been employed to carry out nanoindentation simulations [71].

*Bridging cell method (BCM).* The BCM method decomposes the model into three regions, continuum, bridging, and atomistic domains, and couples them using a finite element (FE) framework [72-75]. A combined FE-molecular mechanics (MM) simulation is employed to discretize the system into atom/nodal centric elements based on the atomic scale FE method [76, 77]. To account for temperature effects, a temperature-dependent interatomic potential, e.g., the one developed by Subramaniyan and Sun [78], can be incorporated. The coupling of the atomistic and continuum domains is realized using the bridging cells, which contain locally formulated atoms whose displacements are mapped to the nodes of the bridging cell elements. BCM has indeed been used for nanoindentation studies [79].

*Concurrent atomistic-continuum (CAC).* The development of the CAC method was motivated by the fact that most concurrent domain decomposition methods do not permit an atomistic-based description of dislocations in the continuum regions, nor do they allow smooth movement of dislocations between the atomistic and continuum regions [80]. In CAC, discontinuous FEs with faces on the slip planes of the lattice, e.g.,  $\{111\}$  planes in face-centered cubic (FCC) and  $\{110\}$  planes in body-centered cubic (BCC) lattices, are employed in the continuum region to accommodate dislocations and intrinsic stacking faults [81]. In the continuum region, all nodes are non-local and the interatomic potential is the only constitutive relation [82, 83]. As a result, there is no ghost force at the atomistic/continuum domain interface [84]. Both static [84] and dynamic [66] formulations of CAC have been developed, the latter of which has been applied to finite temperature nanoindentation problems [67, 85].

*Coupled atomistic/discrete-dislocation (CADD).* The CADD method [86, 87] couples an MD or MS sub-domain to a DDD sub-domain and allows dislocations transition between them. Pad atoms, located on the continuum side of the atomistic/continuum domain interface and deformed with the nodes, are used as an intermediary between the local continuum and the non-local atomistic regions to provide boundary conditions for the latter. In 2D, a detection band is built in the atomistic domain some short distance from the domain interface for monitoring the lattice deformation and to detect atomic-level dislocations, which are then annihilated in the atomistic region accompanied by that the same dislocation is re-built across the interface in the continuum region. Recently, the CADD method has been extended to solve 3D problems, introducing new coupling techniques to pass dislocations in lieu of the detection bands [88-93]; yet it has not been applied to 3D nanoindentation/scratching problems primarily due to some issues in modeling complex dislocation network that is common in the process. Until now, the CADD method [94, 95] has been applied to 2D nanoindentation [65] and nanoscratching [96] at finite temperatures.

*Coupling of length scales (CLS).* A CLS multiscale simulation contains a handshake region where within it, a one-to-one correspondence between MD atoms and FE nodes is obtained even though not all atomic sites are nodal positions [97-100]. The number of FE nodes decreases and the size of the corresponding elements increases while keeping out of the handshake region in the continuum domain. In the MD domain, the dynamics of particles is dominated by their interactions via the interatomic potential, while linear elasticity theory is used for particles in the FE region. The weighted function of an average Hamiltonian developed by Lidorikis and colleagues [97-100], and known as CLS, is utilized for the hybrid atom/node particles. This multiscale technique has been applied to nanoindentation [101].

*Hot-quasicontinuum-dynamic (Hot-QC-dynamic).* The QC method<sup>1</sup>, one of the most popular multiscale modeling approaches, was first developed to simulate static properties of crystalline solids [102]. The crucial phase in developing hot-QC, which extends the static QC to finite temperature setting, is the derivation of an effective Hamiltonian which sufficiently estimates the contributions of the unrepresented atoms in the continuum domain. This can be solved through computing the missing entropy associated with those atoms using a local harmonic or quasi harmonic approximation at the nominal set temperature. In the atomistic region, the dynamics evolves using MD with forces calculated from the effective Hamiltonian at the desired temperature. Based on the way of treating the continuum domain, two types of hot-QC are realized. In “hot-QC-static”, the free energy of the continuum is minimized at each MD time step of the atomistic region. In “hot-QC-dynamic”, equations of motion are introduced for the macroscopic system, so that the system essentially samples configurations close to the one that minimizes the Helmholtz free energy [103, 104]. In the literature, hot-QC-dynamics has been applied to nanoindentation [103, 104].

*Hyper-quasicontinuum (Hyper-QC).* Hyper-QC combines hot-QC (either static or dynamic variants) [103, 104] and hyperdynamics [25], which is a technique for accelerating time in MD simulations, within a single framework. Hyper-QC is able to deal with the long-time simulation of systems which evolve via a sequence of rare, thermally activated, events, yet where the coupling to a long-range strain field is also vital to probe the pertinent physics. For nanoindentation problems, in comparison with the unaccelerated hot-QC which is on the same time scale as classical MD, hyper-QC achieves indentation rates that are close to real experimental values for system sizes that are sufficiently large to preclude boundary effects on atomic-scale mechanisms under the indenter [26, 27].

*Meshless Hermite-Cloud/MD.* Meshless methods are very efficient in simulating strain

---

<sup>1</sup> <http://qcmethod.org/>

localization problems such as nanoindentation/scratching [9, 105]. Meshless Hermite-Cloud/MD multiscale technique uses MD to model the atomistic domain, the strong-form meshless Hermite-Cloud method [106] to model the continuum domain, and a handshaking algorithm to couple these domains. The meshless Hermite-Cloud technique adopts the reproducing kernel particle method (RKPM) [107], the point collocation method, and the Hermite interpolation theorem to achieve an approximate solution for both the field variable and its first-order derivative. In this way, the atomistic-continuum coupling is based on the Schwarz domain decomposition method [108]. This technique has been applied to nanoindentation [109] and nanoscratching [110] at finite temperatures.

*Meshless QC using temperature-related Cauchy-Born (TCB).* The TCB rule [111], which considers the locally harmonic motion of atoms, can be implemented in the QC meshless method to regard the free energy in which temperature effects are involved. Accordingly, the continuum-level stresses computed from the free energy density instead of the strain energy density are temperature-dependent. In this meshless multiscale framework, a background mesh is employed in the element-free Galerkin method (EFGM) [112] and the stress point integration method [113] is adopted to integrate the external nodal forces. Meshless QC using TCB has been used for nanoindentation [111].

*Molecular dynamics/dislocation dynamics/generalized interpolation material point (MD/DD/GIMP).* This multiscale simulation approach couples three different scales, viz., MD at the atomistic scale, DD at the mesoscale, and GIMP [114] at the continuum scale [115], the last of which, a particle-in-cell method, is a generalization of the material point method (MPM) [116-118] which accounts for finite spatial extent occupied by each particle [119]. DD is joined with GIMP via the principle of superposition [120]. Between the MD and DD scales, a detection band seeded in the MD region is applied to pass the dislocations through the boundary using the same method adopted in 2D CADD [87]. To achieve seamless

coupling in simulations at finite temperatures, spatially averaged velocities are utilized to reduce atom vibrations in the transition domain. Note that the heat exchange between MD and GIMP is not allowed and the multiscale scheme is only suitable for isothermal problems. Multiscale simulations using the MD/DD/GIMP technique have been performed to explore nanoindentation [121].

*Multiresolution molecular mechanics (MMM).* The MMM method<sup>1</sup> [122-128] is an energy-based atomistic-continuum coupling technique which employs MM description everywhere in the domain thus does not differentiate between the atomistic and continuum domains. Coarsening is achieved by means of an FE mesh to realize energy approximation by sampling the energies of groups of atoms by only a few selected atoms, and to impose kinematic constraints by using shape functions to interpolate atomic positions from nodal positions. Both static [122] and dynamic [123] forms of MMM have been developed, with adaptive mesh refinement capability. MMM has been employed to investigate 2D [127] and 3D nanoindentation problems [126].

*Other finite temperature multiscale models.* Besides the multiscale modeling methods discussed above, the finite temperature nanoindentation has also been simulated using two other atomistic-based multiscale modeling techniques. In the first model, the dynamics in the atomistic and continuum domains are coupled using displacement boundary conditions and benefits from a linear elastic [129] or quadratic constitutive law [130, 131] in the continuum region to capture nonlinear effects. Thermostating is implemented using the Langevin dynamics with identical damping rate for both the continuum and atomistic domains. In the second multiscale model, an MD domain is merged to a continuum domain characterized by the Young's modulus and the Poisson's ratio [132]. The magnitudes of Young's modulus and the Poisson's ratio are similar to those predicted by the interatomic potential. This helps avoid

---

<sup>1</sup> <https://sites.google.com/site/mmmmethod/>

inconsistencies in the material properties at the interface. The first layer of FEs adjacent to the atomistic region contains a set of imaginary atoms whose function is to allow force continuity between the two regions. This linking allows energy to be transmitted smoothly across the interface [132, 133].

#### **4. Interatomic potential**

As the validity of the atomistic-based modeling results mostly rely on the selection of potential function, precautions are required when choosing interatomic potential for a specific system and process [134-140]. Prior to making intentional selections about which interatomic potential to use, one should ensure that the potential formalism and parameters can accurately capture the required physics and fits for the target problem. For instance, the generalized stacking fault energy (GSFE) surface and elastic constants must be accurately predicted for studies involving the atomic-scale plasticity mechanisms in metals. To examine high temperature solids and high-energy configurations (e.g., a disordered grain boundary (GB)), melting temperature acts as a momentous parameter [141]. Specifically for nanoindentation/scratching at finite temperatures, the interatomic potential should correctly predict the melting temperature and temperature dependent-mechanical properties of materials.

Generally, development of a potential function is an intricate process, the difficulty of which increases with the number of fitting parameters within a given formulation. For a detailed review on the systematic strategy for developing potentials, including general fitting procedures, the development of training sets, discussions of weighting schemes for cost functions, optimization strategies, and approaches to finalizing potentials for the complex systems, readers are directed to the articles by Brenner [142] and Martinez *et al.* [143]. There are a few tools that offer the ability to develop and optimize some interatomic potentials, e.g.,

the General Utility Lattice Program (GULP)<sup>1</sup> [144-146], Design and Analysis Kit for Optimization and Terascale Applications (DAKOTA)<sup>2</sup> [147], and Potential Optimization Software for Materials (POSMat)<sup>3</sup> [148]. Notice that choice of interpolation is also a crucial factor in that even with the correct potential formulation, different interpolation might give different results<sup>4</sup> [149].

## 5. Nanoindentation

The development of finite temperature nanoindentation has provided an opportunity to understand fundamental materials behaviours driven by both temperature and stress. Atomistic-based modeling of finite temperature nanoindentation, though not as abundant as that at zero temperature in the literature, has brought forth important physical insights regarding inherent mechanical properties and deformation propensity of materials at finite temperatures. In the following, we review atomistic-based modeling results in a problem-centric manner to explore the influences of temperature and loading rate on the nanoindentation process.

### 5.1. Effects of temperature

Temperature can affect nanoscale plasticity mechanisms and thermal softening processes acting beneath the indenter, leading to the variation of nanomechanical response of materials at different temperatures. For example, CADD nanoindentation studies of Al, modeled by the embedded-atom method (EAM) potential of Daw and Baskes [150], as seen in Figure 1(a), established that temperature influences the onset of plasticity or dislocation nucleation.

---

<sup>1</sup> <https://gulp.curtin.edu.au/gulp/>

<sup>2</sup> <https://dakota.sandia.gov/>

<sup>3</sup> <https://data.mendeley.com/datasets/shgx2kbr79/1>

<sup>4</sup> <https://openkim.org/>

Temperature rise from 0 to 400 K triggers the earlier occurrence of dislocation nucleation, as demonstrated Figure 1(b), which are in line with the results obtained from the fully atomistic simulations [65]. Interestingly, 2D nanoindentation using MD/DD/GIMP framework reveals that, with a wedge indenter, the onset of dislocations is independent of substrate temperature in the range of 0-300 K, and the load-displacement ( $P$ - $h$ ) curves are found to overlap each other in this temperature range [121].

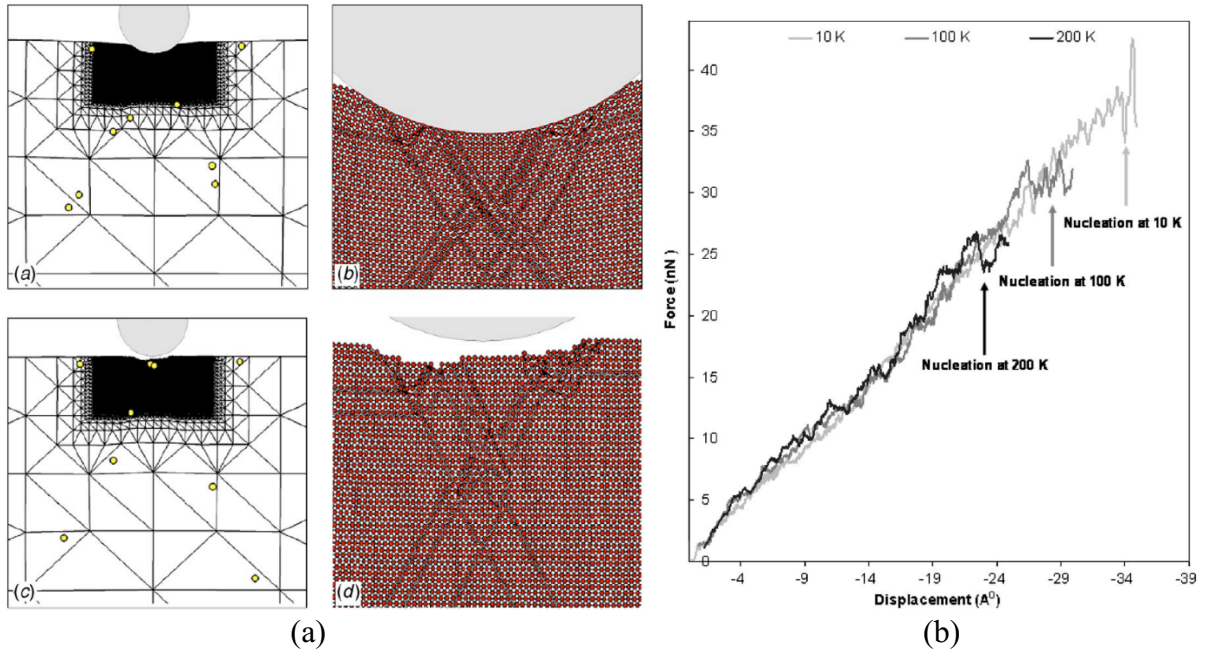


Figure 1 (a) Discrete dislocations (yellow circles) and atomic region at maximum load during and after loading by finite temperature CADD. (b)  $P$ - $h$  curves for three different temperatures. Adopted with permission from Ref. [65].

Figure 2 demonstrates the hot-QC-dynamic simulation model of nanoindentation of Ni, modeled by the EAM potential of Angelo *et al.* [151]. This simulation cell, consisting of 4542 representative atoms, exhibits a significant decrease of the degrees of freedom as opposed to the 790,000 atoms in the equivalent fully atomistic simulation. Hot-QC-dynamic simulations disclose the softening of the  $P$ - $h$  curve, with the nonlinear decrease of critical load for dislocation nucleation with increasing temperature (Figure 2 (b)). This is expected since nucleation of dislocations is a thermally-activated non-linear process [103].

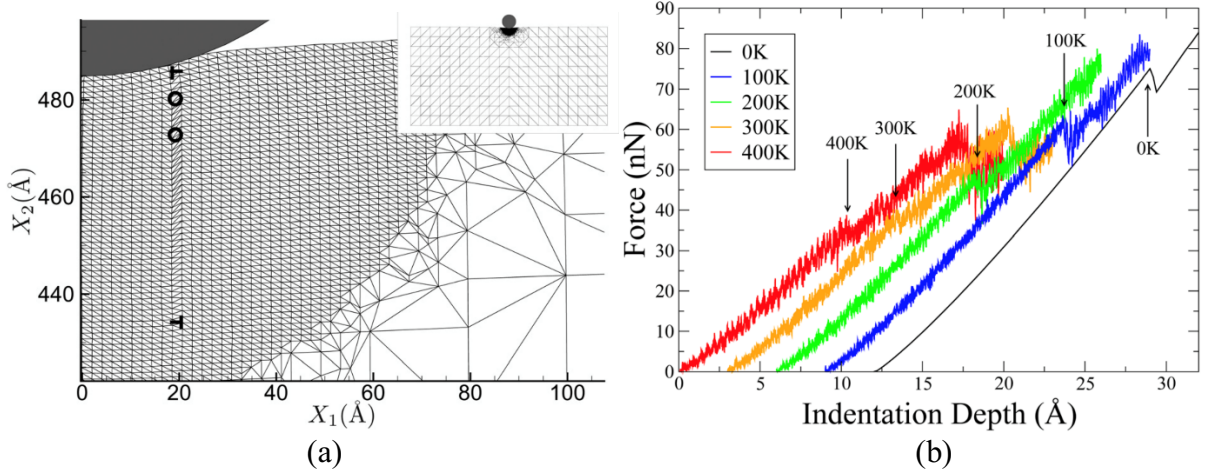


Figure 2 (a) Mesh of the hot-QC-dynamic after dislocation nucleation at  $T=100$  K, (b)  $P$ - $h$  curves. Arrows designate the first nucleation of dislocation. Adopted with permission from Ref. [103].

Multiscale modeling of the nanoindentation of Al [133], modeled by Brenner potential [152, 153], establishes that at 300 K, slip occurs in  $\{111\}$  planes, migrating downward under the indenter. At 650 K, slipped atoms, relative to their neighbours, behave differently compared to those at 300 K. In this case, the atomic motion is more like a viscous flow than slip in well-defined planes and directions [133].

Figure 3 demonstrates the process of dislocation climb of half prismatic loops at 950 K obtained by an MD simulation of nanoindentation of Au on its (111) crystal plane using the EAM potential of Grochola *et al.* [154]. Monoatomic jogs are formed on the dislocation segment and they rapidly climb towards the upper surface, shrinking the loops in a direction parallel to the upper surface which leads to the annihilation of half prismatic edge dislocation loops via pipe diffusion of vacancies from the free surface. Furthermore, the annihilation time and critical loop radius below which pipe diffusion is dominant decrease with increasing substrate temperature [155]. Note that below 800 K, edge dislocation climb is not perceived during MD simulations of Au (111).

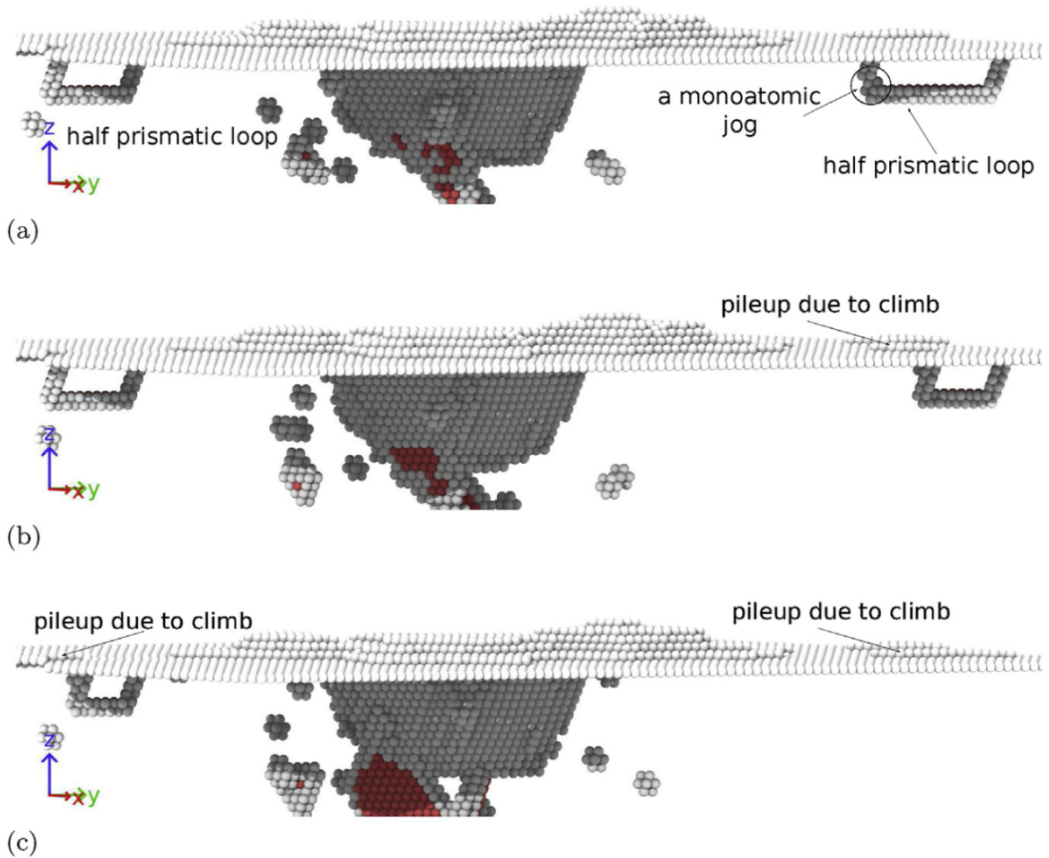


Figure 3 The process of dislocation climb of half prismatic loops at 950 K in the MD simulation of nanoindentation of Au (111). (a) Two in-plane dislocations are shown; (b) The dislocation on the right shrinks, leaving an atomic layer of material pileup on the free surface until complete annihilation on a later stage, as shown in (c); (c) The second in-plane dislocation starts shrinking and annihilates like the first one, leaving an atomic layer of material pileup at the free surface. Adopted with permission from Ref. [155].

High temperatures shift the onset of plasticity, i.e. nucleation of the first dislocation, to a lower indentation depth regime in single crystalline cubic silicon carbide (3C-SiC) substrates, attributable to the thermally-activated nature of defect formation. Figure 4 reveals that intrinsic stacking faults (ISFs), surrounded by Shockley partials, can be formed within the prismatic loops at temperatures higher than 1000 K during nanoindentation of 3C-SiC single crystal. In nanotwinned 3C-SiC samples subjected to nanoindentation loading, it is found that dislocation-coherent twin boundary (CTB) interactions and transmission mechanisms at high temperatures are akin to those at low and room temperatures, i.e. nucleation of twinning partial dislocations and formation and annihilation of point defects at the CTB, suggesting

that the transmission mechanisms are not temperature-dependent [156].

As evident from Figure 5, high temperature nanoindentation of chromium (Cr) and chromium nitride (CrN) coatings [157], modeled by Morse potential function [158], and Ni<sub>3</sub>Al (111) [159], modeled by the EAM potential of Du *et al.* [160], reveal the formation of vacancies, slips and nucleation of dislocations in the material structure prompted by variations in the temperature. In all, these atomistic-based predictions pose interesting questions regarding the apparent role of thermally activated mechanisms during nanoindentation of various materials.

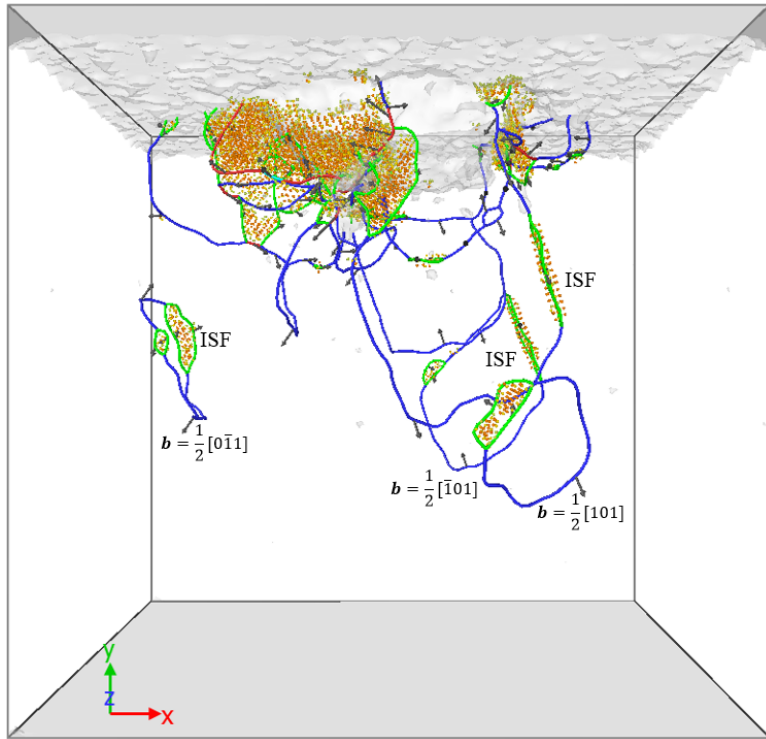


Figure 4 A snapshot showing the formation of ISFs, surrounded by Shockley partials (green lines), within the prismatic loops in the single crystalline 3C-SiC indented at  $T=2000$  K.

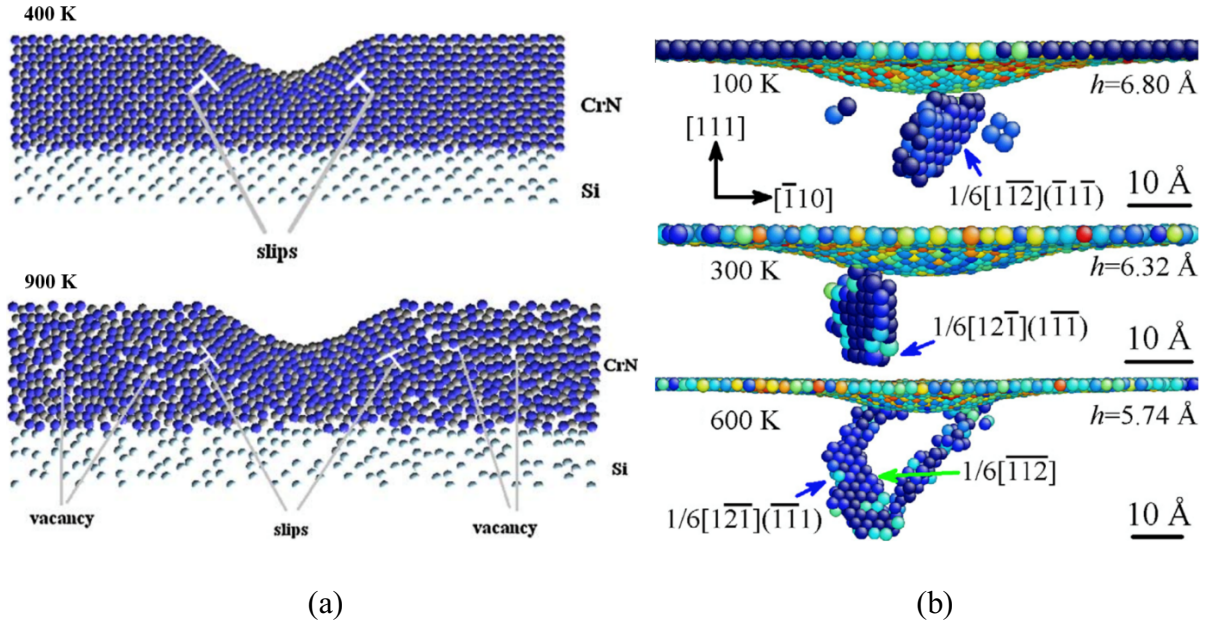


Figure 5 (a) CrN thin film in nanoindentation at 400 K and 900 K, (b) Extended dislocation nucleation at higher temperatures for Ni<sub>3</sub>Al (111). Adopted with permission from Refs. [157, 159].

Besides the plastic deformation mechanism, temperature also affects mechanical properties, e.g., Young's modulus and hardness. Nanoindentation studies by multiscale modeling of CADD [65], AFEM [71], CLS [101], BCM [79], and meshless QC using TCB [111], etc., confirm the deterioration of certain mechanical properties and indentation load with increasing temperature, which have been reported by MD studies as well for a wide range of materials. For example, a higher temperature results in decreasing hardness, Young's modulus and elastic recovery of Cu and Au, modeled by tight-binding-second-moment approximation (TB-SMA) [161] and Morse [162] interatomic potential functions [163-165]; decreasing elastic modulus of the Au and Al [166] using TB potentials [167]; decreasing hardness of nanotwinned single and nanocrystalline 3C-SiC, modeled by Vashishta potential [168], with a more pronounced temperature effects for the nanocrystalline samples [156]; decreasing plastic energy, indentation load, and adhesion of Al/Ni multilayered films [169], modeled by a TB-SMA potential [170]; decreasing load, contact pressure, indentation modulus, and maximum shear stress of Ni<sub>3</sub>Al (111) [159], modeled by the EAM potential of

Du *et al.* [160]; decreasing load, Young's modulus, elastic and plastic energy of the C<sub>60</sub>-filled carbon nanotube (CNT) [171], modeled by Tersoff potential [172-175]; decreasing hardness of Cr and CrN [157]; decreasing load and hardness of cubic boron nitride (cBN) (001) film, modeled by a modified Tersoff potential [176]; as well as decreasing Young's modulus, maximum loading displacement, and load stress of single-layer molybdenum disulphide (MoS<sub>2</sub>), modeled by Stillinger-Weber (SW) [177] and reactive empirical bond order (REBO) [178] interatomic potentials [179, 180]. These decreases of nanoindentation hardness, modulus, and loads with increasing temperature may be attributed to the increase of the amplitude of atomic vibration, which leads to thermal expansion and reduces the energy needed to change the atomic bonds. It is informative to note that the nanomechanical response of materials at elevated temperatures qualitatively interprets the usefulness of heated array of tips in indenting or a heated mold in stamping a fairly soft material, which can be crucial to the mechanisms involved in nanofabrication processes, e.g., nanoimprint lithography technologies [165].

In addition to the crystalline materials, the material behaviour of amorphous compounds, e.g., bulk metallic glasses (BMGs), subjected to nanoindentation is also of interest. Prior MD nanoindentation studies have brought into attention some important features on the mechanistic aspect of these alloys drawing examples on Ni<sub>50</sub>Zr<sub>50</sub> modeled by TB-SMA potential [181]. For temperatures around and above the glass transition temperature ( $T_g$ ) of Ni<sub>50</sub>Zr<sub>50</sub>, i.e.  $\sim 748$  K, the nanoindentation hardness does not decrease with increasing temperature. In fact, the hardness and slip vector distribution do not vary in the temperature range of 700 K to 900 K, plausibly due to the change of material state from solid to high-viscosity liquid [182]. From the perspective of free volume theory [183-185], during the formation process of metallic glasses, there is necessarily ample free volume in their structure. When the simulation temperature rises, the motion of atoms is intensified.

Accordingly, the free volume slowly decreases and atoms rearrange, gradually forming ordered regions. Following above, the motion and migration of atoms are limited to a small region and the increase of shear transformation zones (STZs) results in the tendency to rise of elastic modulus. However, when free volume decreases to a certain degree, where atoms become random-close-packed and their motion is limited, the development of STZs is restrained. This causes fluctuation of material properties and the decrease of elastic modulus. Afterwards, when the temperature continues to rise, there is further release of energy between atoms. Meanwhile, the free volume begins to expand and the motion of atoms is motivated to become active again. At the same time, the size of STZs starts increasing again. Finally, as the temperature surpasses  $T_g$ , STZs constantly form and grow, tending to expand and consequently the elastic modulus increases rapidly under the effect of these tiny STZs. Thus, as the temperature gradually rises, the elastic modulus of the substrate tends to change, which is mainly due to the effect of STZs and the change of the free volume. Such behaviour have been observed for the metallic glass Cu<sub>50</sub>Zr<sub>50</sub> [186] modeled by an EAM potential [187], and Ni<sub>70</sub>Al<sub>30</sub> alloy [188] modeled by a TB potential [167]. On the whole, metallic glasses have features of rubber and protein like materials, and behave differently compared to the regular metals and alloys, i.e., they become stiffer before glass transition [189].

It is instructive to mention that the nanoindentation hardness and Young's modulus obtained by atomistic-based simulations are higher than the experimental magnitudes, albeit a quantitative agreement is realized. This discrepancy could stem from the: high loading rates in MD, indentation size effect (ISE), dissimilar crystal texture used in MD and experiment, true contact area issues, limited dislocation activity in MD due to specimen scales and the experimental scatter and surface roughness in experimental specimens.

## 5.2. Effects of loading rate

The hyper-QC simulations of single crystal Ni reveal a thermally activated nucleation process where the force required to nucleate the first partial dislocation is logarithmically dependent on both the temperature and indenter velocity. The results from hyper-QC, hot-QC, and fully atomistic MD simulations could collapse onto a single curve derived from a simple mathematical model based on thermal activation and linear relations. Notice that in the hyper-QC model, the reduction of the indenter velocity by three orders of magnitude relative to unaccelerated hot-QC simulations is enabled by the introduction of a novel mechanism-based bias potential designed to accelerate the dislocation nucleation process [26, 27].

Different dislocation structures are formed under indenter during nanoindentation of Cu, modeled by the Mishin EAM potential [190], at 900 K at different loading rates. Figure 6 demonstrates the dislocation arrangement generated after the first large load drop for the slow loading rate ( $4.89 \times 10^{-3} \text{ \AA}/\tau$ ) revealed by DMD [23], where the surface step offers favoured sites for heterogeneous dislocation nucleation nearby surface defects. This behaviour is considerably different from that of the faster rate case ( $4.89 \times 10^1 \text{ \AA}/\tau$ ), depicted in the inset of Figure 6 (a), where dislocation loops are formed homogeneously inside the bulk. Indentation load also decreases with decreasing loading rate [23]. Likewise, Meshless Hermite-Cloud/MD studies of nanoindentation of Cu, modeled by Morse potential of Inamura *et al.* [191], reveal decrease of indentation load with the decrease of loading rate [109, 192].

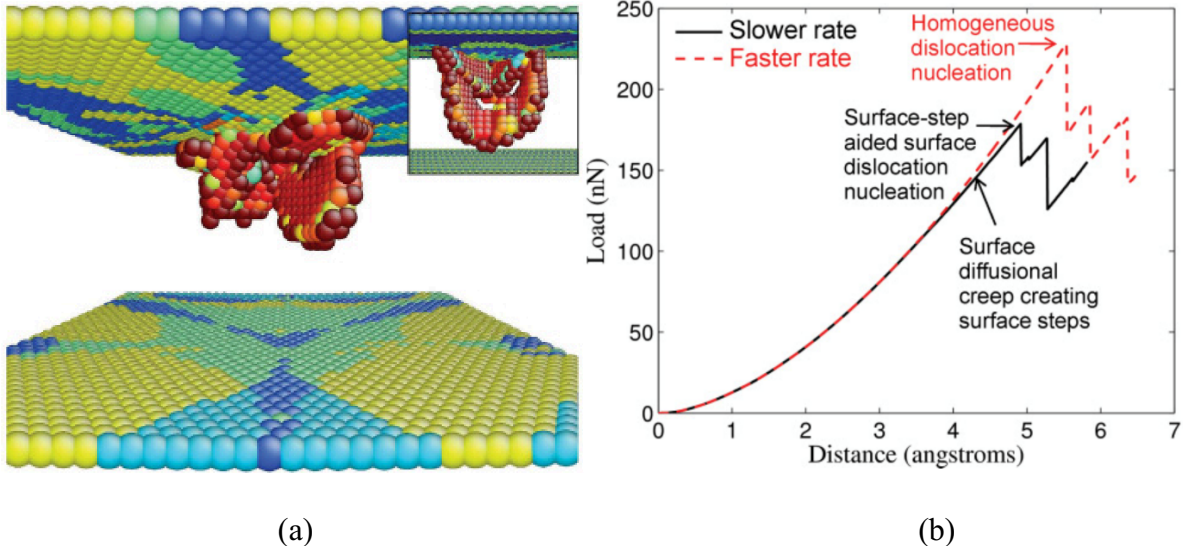


Figure 6 Effects of loading rate on dislocation structure revealed by DMD. (a) Dislocation nucleation at low loading rate, and high loading rate (in the inset), (b)  $P$ - $h$  curve demonstrates reduced dislocation nucleation load as a result of the surface vacancy disk/terrace generated by prior diffusion. Adopted with permission from Ref. [23].

Low indentation speeds, e.g., 5 and 10 m/s, bring about a more homogenous nucleation and propagation of lattice dislocations in the nanotwinned single crystalline 3C-SiC than those of higher indentation speeds. Also, a careful examination of the evolving dislocation structure under the indenter uncovers that the onset of plastic deformation is delayed at higher indentation speeds. In nanotwinned nanocrystalline 3C-SiC, GB and CTB accommodation processes along with low dislocation activity are found as the mediators of the plasticity at low indentation speeds up to 50 m/s, however, at higher speeds, i.e., 100 m/s, the contribution of GB sliding and CTB migration is more pronounced. Detailed analysis of the indentation hardness unravels that hardness increases with the indentation speed in nanotwinned single/nanocrystalline 3C-SiC, however, a slight decrease transpires for the nanotwinned nanocrystalline sample while increasing the indentation speed from 50 to 100 m/s, which may be attributed to the improved GB sliding at high indentation speeds. Another remarkable point is that decreasing the indentation speed lowers the onset of plasticity of the nanotwinned single crystals, i.e. pop-in load reduces by ~29% and ~32% when decreasing the

indentation speed from 100 to 5 m/s [156].

## 6. Nanoscratching

Almost all the literature on the multiscale modeling of nanoscratching is centered on discussions of zero temperature nanoscratching [193-198]. On the other hand, the available literature reveals that MD simulation of nanoscratching has been primarily concentrated in demystifying the occurring mechanisms at room temperature. Thus, the current pool of knowledge on high/finite temperature nanoscratching is sparse. Accordingly, there are tremendous opportunities to develop/adopt finite temperature multiscale models and high temperature MD simulations to explore the overall response of materials under nanoscratching conditions and to perform parametric studies on state variables which are experimentally difficult to access. On the basis of existing literature, we present parameter-specific case studies of nanoscratching studies in this section.

### 6.1. Effects of temperature

An MD study of plastic deformation mediated flow behaviour of single crystalline Si and 3C-SiC reveals that the rotational flow of atoms beneath the indenter/cutting tool diminishes linearly when the temperature of substrate increases [199, 200], as demonstrated in Figure 7, plausibly owing to the occurrence of thermal softening which, in turn, improves the plasticity of the substrate. The atomic flow in the substrate is a laminar flow at room temperature whilst at higher temperatures the flow of the material is seemingly turbulent. Also, it is found that thinner and taller chips (pile-up) form and deformation layer depth in the substrate becomes greater under high temperature conditions. Moreover, shear plane angle increases while scratching/cutting at high temperatures, signifying that shear plane has a smaller area, thus, shear occurs in a more narrowed zone leading to lower shear forces [200, 201]. Decrease of

critical von Mises stress triggering flow, and scratching/cutting forces with increasing substrate temperature have also been reported for Si [200], 3C-SiC [202], and metallic glass NiAl [203].

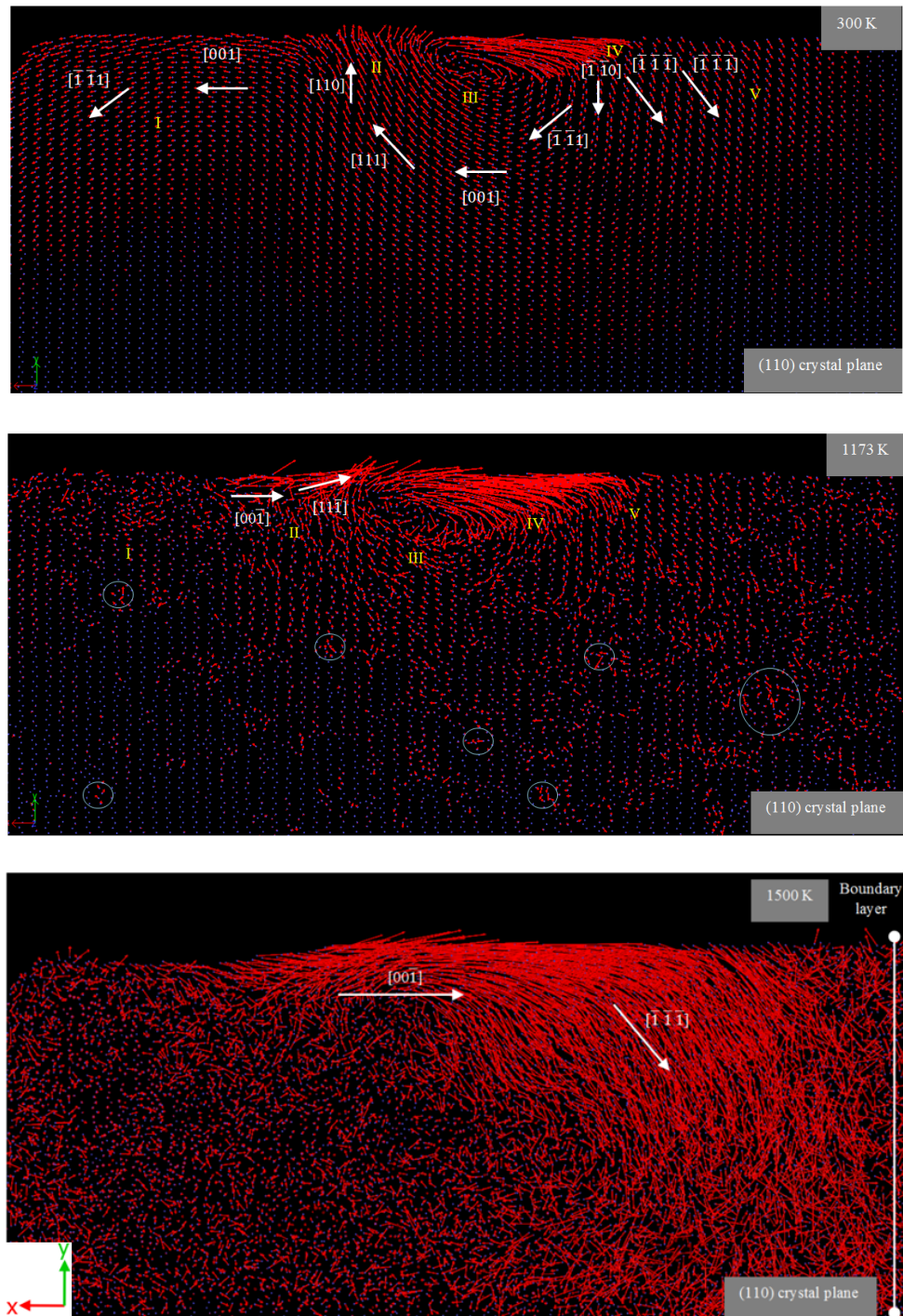


Figure 7 Atomic flow field obtained in nanoscratching/cutting of Si(110) at various temperatures. The red arrows demonstrate displacement vectors of atoms with their lengths indicating the amount of displacement. Highly distorted atoms are highlighted by grey

circles. The vertical line in the last subfigure denotes the boundary layer. Adopted with permission from Ref. [199].

MD simulation studies of nanoscratching/cutting of Si using SW potential function [204] have recently revealed the stochastic formation of dislocations and stacking faults at various temperatures, where perfect  $60^\circ$  dislocations prevail perfect screw dislocations and partial dislocations. In 3C-SiC, modeled by analytical bond order potential (ABOP) [205], formation and subsequent annihilation of stacking fault-couple and Lomer-Cottrell (L-C) lock at high temperatures, i.e. 2000 K, could occur. Additionally, cross-junctions between pairs of counter stacking faults mediated by the gliding of Shockley partials on different slip planes are formed at 3000 K during nanoscratching/cutting of the 3C-SiC(110)<001> crystal setup [206]. Such results are particularly beneficial, in that they provide a strong physical argument for the genesis of the mechanisms involved in crystal plasticity of Si at high temperatures. Given the development of a new potential function for Si by Pun and Mishin [207], and Vashishta potential function [168] for the 3C-SiC, which can accurately reproduce a great variety of properties including GSFE, it is worthwhile to revisit the defect formation of these materials under localized strain problems at elevated temperatures using these potential functions.

A well-known approach to quantify crystals in MD simulation is the virtual X-ray diffraction (XRD) developed by Coleman *et al.* [208]. Using this technique, it is established that the intensity peaks are not shifted at higher temperatures before nanoscratching/cutting of Si and 3C-SiC, suggesting that interplanar spacings do not change. Nevertheless, main peaks are abated significantly after scratching/cutting, and numerous new diffractions emerge, signifying the occurrence of a transformation towards an amorphous configuration in the scratching/cutting region [206, 209].

Besides the effects on plasticity, the temperature also influences the nanoscratching process

from which much nanotribology information that is not available in nanoindentation (Section 5.1) can be obtained. Zykova-Timan and co-workers [210] have conducted an interesting MD study showing a frictional drop close to melting point of NaCl (100), modeled by the classic Born-Mayer-Huggins-Fumi-Tosi (BMHFT) two-body potential [211, 212], for deep ploughing and wear. In contrast, an increase of friction for grazing, wearless sliding is achieved. As shown in Figure 8, for deep ploughing and wear, a frictional drop as in skating close to melting point takes place, whereas a frictional rise as in flux lattice depinning for grazing, wearless sliding occurs. Meticulous inspection of the contact zone reveals that the sharp tip resembles a skate on an ice rink, where the surface is locally molten: the sharp tip is accompanied by a small fluid cloud and skates on the hot NaCl surface. Ostensibly, the scale of these interning phenomena can be relevant to future MEMS/NEMS made by Si. Although the choice of NaCl for the MD simulations appears more academic, the disappearance of friction phenomenon might happen on other non-melting surfaces, e.g., Al (111) or Pb (111). Hence, the work evidently directs attention to the ploughing configuration as a goal to attain minimum friction in high temperature applications [213]. However, the melt lubrication process imposes a dilemma, i.e., diminishing the surface strength as opposed to the nearly zero friction surface. It appears that the predictions of Zykova-Timan and colleagues [210] correlate with the previously reported results in the 1990s regarding the use of liquid metals for friction reduction [214, 215]. Nonetheless, experiments show that the friction behaviour upon melting may depend on the alloy composition [216]. By and large, it is enticing to perform high temperature and high velocity nanoscale studies to further explore the influence of liquid film formed at the interface upon melting on the frictional behaviour.

Another crucial point is that high temperature nanoscratching enhances plastic deformation of substrate which directs us to expect lower wear of diamond indenter. However, it should be bore in mind that high heat content could lead to wear of diamond indenter, viz., high

temperature can prompt accelerated wear of carbon atoms via diffusion, attrition, adhesion, etc. Given the importance of this topic, it is worthwhile to examine the wear mechanisms and phase transformation of the indenter at elevated temperatures using atomistic-based simulations in vacuum as well as in the presence of oxygen atoms, which could potentially suggest ways to improve wear resistance and to propose new materials/coatings for high temperature applications.

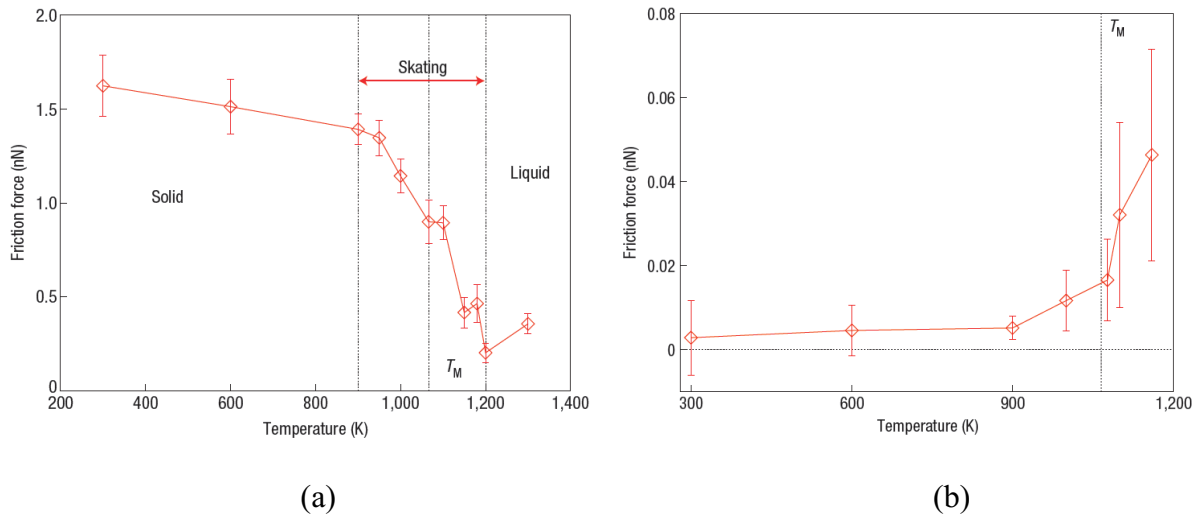


Figure 8 Nanofrictional force of (a) Ploughing, (b) Grazing tip on NaCl (100). Near melting temperature  $T_M$ , friction drops as in skating for the sharp (ploughing) tip whereas the blunt tip, grazing on the surface, experiences an increase in friction. Adopted with permission from Ref. [210].

## 6.2. Effects of scratching speed and depth

The tangential and normal forces are dependent to the scratching speed and depth. As revealed by CADD [96], the average magnitude of normal forces of the Al substrate, modeled by EAM potential of Daw and Baskes [150], increases rapidly at scratching speeds over the propagation speed of plastic wave. As depicted in Figure 9, the average normal force decreases up to the scratching speed of 400 m/s, followed by a sudden rise at 800 m/s. This trend could be attributed to the transition from crystal plasticity owing to lattice dislocation motion to an amorphization process, which might be related to the loss of lattice stability in

CADD simulations. Also, much smoother surface is obtained while scratching at high speeds. However, the outcome from Meshless Hermite-Cloud/MD of Cu [110] contradicts the findings from the CADD [96], i.e., the tangential and normal forces increase with increasing scratching speed in the range of 10-400 m/s.

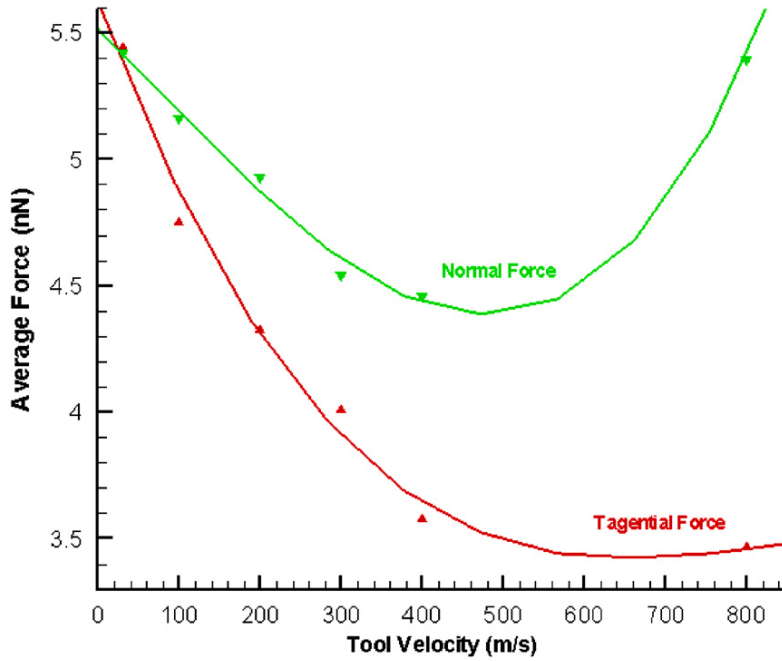


Figure 9 Variation of average tangential and normal forces with scratching speed during nanoscratching of Al obtained by CADD. Adopted with permission from Ref. [96].

Meshless Hermite-Cloud/MD [110] and CADD [96] studies of Cu an Al, respectively, at room temperature demonstrates a linear increase of normal and frictional forces with increasing scratch depth, yet the coefficient of friction remains almost constant [110]. As depicted in Figure 10(a), CADD studies of tangential force curve reveal huge drops at certain points, corresponding to the nucleation of some dislocations shown in Figure 10(b) and Figure 10(c). Larger scratching depth would also trigger higher levels of dislocation nucleation and plastic deformation ahead of the indenter [96].

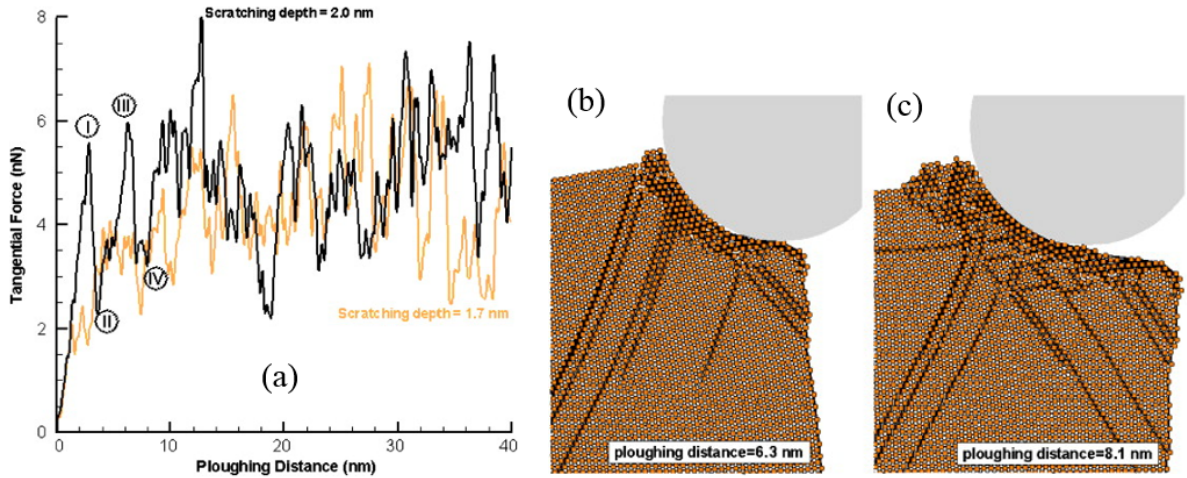


Figure 10 (a) Variation of tangential force as a function of scratching depth. Points *I-IV* correspond to dislocation nucleation events; (b) and (c) Dislocation nucleation between points *III* and *IV* shown in (a). The results were obtained by CADD. Adopted with permission from Ref. [96].

### 6.3. Effects of cutting plane/direction

The mode of nanoscale plasticity at different temperatures is cutting plane/direction-dependent, e.g., in Si and 3C-SiC, while low defect activity transpires for the (010)[100] and (111)[ $\bar{1}$ 10] crystal setups, formation of dislocations and stacking faults prevails during scratching/cutting the (110)[00 $\bar{1}$ ], attributable to the ease of activating slip systems in this crystal setup [206, 209]. In the former cases, amorphization and weak bonding between atoms govern the plasticity at high temperatures. Additionally, regardless of the temperature, the stacking faults, which are not formed for both the (010)[100] and (111)[ $\bar{1}$ 10] crystal setups, are generated with three atomic layers in the (110)[00 $\bar{1}$ ] during scratching/cutting of Si [209]. Detailed analysis of atomic flow demonstrates that while scratching/cutting (111) crystal plane, the center of rotational flow, shown in Figure 7, locates at a lower position than those on the other crystal planes, thus, providing a more effective flow of the atoms which eases the material removal process. For this crystal plane, irrespective of temperature, the stagnation region, where the shearing action (leading to chip formation) separates from the compressive action beneath the indenter, is located at an upper position than that for the (010)

and (110) orientations, signifying that ploughing due to compression is relatively higher on the (111) plane and thus the extent of deformed surface and subsurface, leading to higher spring-back, is more pronounced for this orientation [199]. Besides, smaller critical von Mises stress, resultant force, and friction coefficient at the indenter/chip interface is visible while scratching/cutting the (111) surface, as opposed to surfaces on other crystallographic planes [200-202].

## 7. Summary and outlook

The role of modeling and simulation has become crucial in the growth of nanomechanics and nanotribology, in which microscopic processes are experimentally inaccessible, to make momentous predictions and reveal hitherto unknown phenomena. In particular, modeling of the nanomechanical responses of materials systems and deformation mechanisms of surface atoms in contact regions of MEMS/NEMS under various forms of loading at service temperatures are of relevance to industrial application. Of the wide variety of materials characterisation techniques, nanoindentation/scratching is one of the most rigorous approaches to gain information about local material properties, as well as fundamental deformation mechanisms. Accordingly, modeling of nanoindentation/scratching at finite temperatures opens up significant new possibilities, shedding light on the fundamental mechanisms of surface plasticity and the tribological behaviour of thin films. Two types of atomistic-based modeling approach have primarily been pursued to explore finite temperature nanoindentation/scratching of materials – MD simulation and atomistic-based multiscale modeling. Meanwhile, it is critical to ensure that the interatomic potential formalism used in MD and multiscale modeling accurately captures the relevant physics. Specifically for finite temperature nanoindentation/scratching, the selected interatomic potential ought to precisely predict melting temperature, temperature-dependent mechanical properties, GSFEs, and point

defect structures at finite temperatures. Development of long-range interatomic potentials and formalisms with higher levels of transferability, i.e., capability of accurately predicting mechanical and thermal properties as well as defect and dislocation core structures of materials at high temperatures, is promising.

Fewer MD simulations have been carried out for nanoindentation at high temperatures ( $> 300$  K) than those at lower temperatures, and most of them focused on investigating the variation of modulus, hardness, and elastic recovery with temperature. The discovery of deformation modes and nanopl plasticity mechanisms acting beneath the indenter at high temperatures, as well as material flow behaviour, require further examination in order to ascertain the role of deformation phenomena on the nanomechanical responses of different materials systems such as multi-layered films, nanocrystalline materials, polycrystalline structures, and nanocomposites at elevated temperatures. Also, from the MD simulation assessment, one can examine the influence of oxide layers on the nanomechanical behaviour of thin films at high temperatures. To that end, oxygen atoms should be included in the MD models and robust potential functions have to be used to describe interatomic interactions between oxygen atoms and other atoms in the system. It also remains to be seen how temperature affects the defect formation mechanisms involved in nanopl plasticity of semiconductor materials upon nanoindentation/scratching loading, which will assist in enhancing our understanding of physical response of these materials. Specifically, the ongoing debate regarding the occurrence of high pressure phase transformation (HPPT) in Si and the role of temperature on the rate of HPPT at a strictly nanometre level and defect-free sample employed in MD trials could benefit from further atomistic calculations. It is worth noting that as empirical interatomic potentials are parameterized for a particular local environment of atomic configurations, they are generally not designed for conditions where the number of interacting neighbours can alter suddenly, e.g., during nanoindentation/scratching loading.

Thus, interatomic potentials like Tersoff [172-175], being a nearest-neighbour model, are expected to become aphysical in the high pressure regime when the second-neighbours come within the range of what was defined to be the first-neighbour range [217]. It is, therefore, vital to ensure that the employed interatomic potential is reliable in describing and capturing all the structural phases of Si at different temperatures. Besides nanoindentation, very few MD studies on high temperature nanoscratching/cutting have been reported in the literature. More research on this topic is likely to appear in the coming years.

From a multiscale modeling perspective, a review of the available literature reveals that the complicated but very promising atomistic-based multiscale models for finite temperature nanoindentation/scratching, capable of passing dislocation and heat between atomistic and continuum domains, offer a unique alternative to overcoming the spatial limitations of MD. Nevertheless, it should be considered that MD plays a central role in multiscale modeling and, indeed, is employed as a fundamental basis in most multiscale modeling approaches. Particularly, accelerated MD schemes, e.g., hyperdynamics [25], parallel replica method [218], temperature-accelerated dynamics [219], which aim to tackle the restricted time scale accessible in conventional MD simulations, can be incorporated into atomistic-based multiscale methods to speed up simulations. Nevertheless, it should be borne in mind that MD is not a very reliable choice for non-equilibrium high temperature simulations in metals/metallic superalloy, metallic glasses, and some high-conductivity semiconductors, since electrons (which cannot be modelled in classical MD) dominate heat transfer in them, but not in insulators, e.g., carbon. For quasi-static, zero temperature problems, multiscale techniques are well understood and developed. However, multiscale methods encounter sizeable challenges at high temperatures because of the incompatible interface stemming from non-local atomic and local continuum descriptions. This artificial interface induces the ghost forces and spurious phonon reflection, which trigger the temperature gradient and

seriously interfere with the dynamical equilibrium in the entirely coupled model. This can be termed as the greatest challenge for developing high temperature multiscale models. Notice that in experimental systems, rapid vibrations would be converted to heat by viscoelastic damping in the solid or incoherent scattering at boundaries or impurities. The key goals of developing high temperature multiscale models for nanoindentation/scratching should therefore include restricting spurious reflections at artificial boundaries such as the handshake region and minimise reflections at real boundaries by damping waves or ensuring that scattering is incoherent. Some recently developed algorithms can reduce reflections at the boundaries of atomistic regions, yet transmission of crucial low-frequency strain waves might also be influenced and these remain limited to linear constitutive laws. Moreover, the use of non-linear constitutive law in the continuum domain is highly recommended because non-linear effects become substantial at strains of about 0.3%, and compressive strains imposed by the indenter remain above this level far below the surface [130]. An ambitious goal would be developing physics-based crystal plasticity [220, 221] models capable of capturing the hardening/softening effects, lattice rotation, and texture evolution encountered in materials by incorporating linear and planar defects (e.g., dislocations, stacking faults, twinning, GBs) in the continuum domain in order to accurately capture the deformation behaviour of materials [222]. Implementing dynamic remeshing algorithms which expand or shrink the atomistic region in response to changing stresses also poses promising future endeavours. In addition, many existing multiscale approaches are only suitable for 2D simulations. 3D dynamic multiscale methods need to be developed for high temperature nanoindentation/scratching. Research on multiscale methods combining meshless or particle techniques for continuum discretisation and the MD method for finite temperature nanoindentation/scratching are also very promising [223-225]; yet a few efforts in this direction has focused on static limits. It is possible to confidently predict intensified research in the arena of finite temperature

meshless/particle-based multiscale methods comprising dislocations, which may be used in many contact problems. To further improve the fidelity of multiscale modeling, atomic dynamics needs to include quantum effects, e.g., zero point energies and non-classical phonon scattering, and trajectories involving excited electronic states in insulators (including transitions between states and effects such as avoided crossings) [31]. Also, multiphysics models that incorporate fundamental understanding and parameters derived from MD and quantum mechanical calculation can provide a powerful approach to nano/microstructural evolution of materials under nanoindenter [28]. It can be concluded that research into multiscale modeling of nanoindentation/scratching at finite temperatures is in its infancy. In the upcoming years, we will become acquainted with more fundamental knowledge about consistent thermodynamics in the continuum-atomistic coupling scheme. The future of multiscale modeling of nanoindentation/scratching at finite temperatures is therefore very promising and more applications remain to be conducted.

It should be emphasized that one of the most interesting and relevant topics to which MD and multiscale modeling of high temperature nanoscratching can be applied is nanotribology at high temperatures. Such studies enhance our understanding about the frictional behaviour of different materials and compounds at high temperatures, particularly around melting temperatures, where Zykova-Timan and colleagues [210] reported a drastic frictional drop upon melting. High temperature nanotribological studies could therefore aid in determining regimes for ultra-low friction and near-zero wear. MD and multiscale simulation studies can also shed light on the atomic origins of wear mechanisms, adhesion, friction, and phase transformation of indenters at elevated temperatures in vacuums as well as in the presence of oxygen, which could suggest ways to improve wear resistance and propose new materials/coatings for high temperature applications. Finally, a one-to-one comparison between modeling and experimental approaches is lacking, primarily because of length/time

scale issues and the application of pristine, defect-free samples in modeling [226]. In our opinion, atomistic-based multiscale methods offer the best hope for bridging the traditional gap that exists between experimental and theoretical approaches and computational modeling for studying and understanding the materials responses under nanoindentation/scratching.

## **Acknowledgment**

SZC would like to express his sincere gratitude for the financial support from the BIAM-Imperial Centre for Materials Characterisation, Processing and Modelling at Imperial College London. The work of SX was supported in part by the Elings Prize Fellowship in Science offered by the California NanoSystems Institute (CNSI) on the UC Santa Barbara campus. SX also acknowledges support from the Center for Scientific Computing from the CNSI, MRL: an NSF MRSEC (DMR-1121053). This work used the Extreme Science and Engineering Discovery Environment (XSEDE), which is supported by NSF grant number ACI-1053575.

## References

1. E. Broitman: Indentation Hardness Measurements at Macro-, Micro-, and Nanoscale: A Critical Overview. *Tribology Letters*. **65**, 23 (2017).
2. S.Z. Chavoshi and S. Xu: Temperature-dependent nanoindentation response of materials. *MRS Communications*. **8**, 15-28 (2018).
3. S.Z. Chavoshi and S. Xu: A review on micro- and nanoscratching/tribology at high temperatures: instrumentation and experimentation. *Journal of Materials Engineering and Performance*. **In Press**, doi: 10.1007/s11665-018-3493-5 (2018).
4. R.W. Carpick and M. Salmeron: Scratching the surface: fundamental investigations of tribology with atomic force microscopy. *Chemical reviews*. **97**, 1163-1194 (1997).
5. R. Consiglio, N. Randall, B. Bellaton, and J. Von Stebut: The nano-scratch tester (NST) as a new tool for assessing the strength of ultrathin hard coatings and the mar resistance of polymer films. *Thin Solid Films*. **332**, 151-156 (1998).
6. T. Tsui, G. Pharr, W. Oliver, Y. Chung, E. Cutiongco, C. Bhatia, R. White, R. Rhoades, and S. Gorbatkin. Nanoindentation and nanoscratching of hard coating materials for magnetic disks. in *MRS Proceedings*. Cambridge Univ Press (1994).
7. S. Xu, J. Rigelesaiyin, L. Xiong, Y. Chen, and D.L. McDowell, Generalized continua concepts in coarse-graining atomistic simulations, in *Generalized Models and Non-classical Approaches in Complex Materials 2*. 2018, Springer. p. 237-260.
8. W.A. Curtin and R.E. Miller: Atomistic/continuum coupling in computational materials science. *Modelling and simulation in materials science and engineering*. **11**, R33 (2003).
9. H.S. Park and W.K. Liu: An introduction and tutorial on multiple-scale analysis in solids. *Computer methods in applied mechanics and engineering*. **193**, 1733-1772 (2004).
10. C.J. Ruestes, I.A. Alhafez, and H.M. Urbassek: Atomistic Studies of Nanoindentation—A Review of Recent Advances. *Crystals*. **7**, 293 (2017).
11. S. Huang and C. Zhou: Modeling and Simulation of Nanoindentation. *JOM*. **69**, 1-8 (2017).
12. D. Sholl and J.A. Steckel, *Density functional theory: a practical introduction*. John Wiley & Sons (2011).
13. J. Li, A.H. Ngan, and P. Gumbsch: Atomistic modeling of mechanical behavior. *Acta Materialia*. **51**, 5711-5742 (2003).
14. R. Elber and M. Karplus: A method for determining reaction paths in large molecules: application to myoglobin. *Chemical Physics Letters*. **139**, 375-380 (1987).

15. G. Henkelman and H. Jónsson: Improved tangent estimate in the nudged elastic band method for finding minimum energy paths and saddle points. *The Journal of chemical physics*. **113**, 9978-9985 (2000).
16. G. Henkelman, B.P. Uberuaga, and H. Jónsson: A climbing image nudged elastic band method for finding saddle points and minimum energy paths. *The Journal of chemical physics*. **113**, 9901-9904 (2000).
17. T. Zhu, J. Li, X. Lin, and S. Yip: Stress-dependent molecular pathways of silica–water reaction. *Journal of the Mechanics and Physics of Solids*. **53**, 1597-1623 (2005).
18. T. Zhu, J. Li, and S. Yip: Atomistic study of dislocation loop emission from a crack tip. *Physical review letters*. **93**, 025503 (2004).
19. G. Sutmann: Classical Molecular Dynamics.
20. M.P. Allen: Introduction to Molecular Dynamics Simulation.
21. U. Landman, W. Luedtke, N. Burnham, and R. COLTON: Atomistic mechanisms and dynamics of adhesion, nanoindentation, and fracture. *Science*. **248**, 454-461 (1990).
22. W.G. Hoover, A.J. De Groot, C.G. Hoover, I.F. Stowers, T. Kawai, B.L. Holian, T. Boku, S. Ihara, and J. Belak: Large-scale elastic-plastic indentation simulations via nonequilibrium molecular dynamics. *Physical Review A*. **42**, 5844 (1990).
23. J. Li, S. Sarkar, W.T. Cox, T.J. Lenosky, E. Bitzek, and Y. Wang: Diffusive molecular dynamics and its application to nanoindentation and sintering. *Physical Review B*. **84**, 054103 (2011).
24. X. Sun, M. Ariza, M. Ortiz, and K. Wang: Acceleration of diffusive molecular dynamics simulations through mean field approximation and subcycling time integration. *Journal of Computational Physics*. **350**, 470-492 (2017).
25. A.F. Voter: A method for accelerating the molecular dynamics simulation of infrequent events. *The Journal of chemical physics*. **106**, 4665-4677 (1997).
26. W. Kim and E. Tadmor: Accelerated quasicontinuum: a practical perspective on hyper-QC with application to nanoindentation. *Philosophical Magazine*. 1-33 (2017).
27. W.K. Kim, M. Luskin, D. Perez, A. Voter, and E. Tadmor: Hyper-QC: An accelerated finite-temperature quasicontinuum method using hyperdynamics. *Journal of the Mechanics and Physics of Solids*. **63**, 94-112 (2014).
28. W. Gerberich, E.B. Tadmor, J. Kysar, J.A. Zimmerman, A.M. Minor, I. Szlufarska, J. Amodeo, B. Devincre, E. Hintsala, and R. Ballarini: Case studies in future trends of computational and experimental nanomechanics. *Journal of Vacuum Science & Technology A: Vacuum, Surfaces, and Films*. **35**, 060801 (2017).
29. M. Arndt and M. Griebel: Derivation of higher order gradient continuum models from atomistic models for crystalline solids. *Multiscale Modeling & Simulation*. **4**, 531-562 (2005).

30. P. Aubertin, J. Réthoré, and R. De Borst: Energy conservation of atomistic/continuum coupling. *International journal for numerical methods in engineering*. **78**, 1365-1386 (2009).

31. D.W. Brenner: Challenges to marrying atomic and continuum modeling of materials. *Current Opinion in Solid State and Materials Science*. **17**, 257-262 (2013).

32. D. Rodney, A. Tanguy, and D. Vandembroucq: Modeling the mechanics of amorphous solids at different length scale and time scale. *Modelling and Simulation in Materials Science and Engineering*. **19**, 083001 (2011).

33. M.F. Horstemeyer, Multiscale modeling: a review, in *Practical aspects of computational chemistry*. 2009, Springer. p. 87-135.

34. R.E. Miller and E.B. Tadmor: A unified framework and performance benchmark of fourteen multiscale atomistic/continuum coupling methods. *Modelling and Simulation in Materials Science and Engineering*. **17**, 053001 (2009).

35. J. Fish: Bridging the scales in nano engineering and science. *Journal of Nanoparticle Research*. **8**, 577-594 (2006).

36. D.D. Vvedensky: Multiscale modelling of nanostructures. *Journal of Physics: Condensed Matter*. **16**, R1537 (2004).

37. N.M. Ghoniem, E.P. Busso, N. Kioussis, and H. Huang: Multiscale modelling of nanomechanics and micromechanics: an overview. *Philosophical magazine*. **83**, 3475-3528 (2003).

38. R.E. Miller and E.B. Tadmor: Hybrid continuum mechanics and atomistic methods for simulating materials deformation and failure. *MRS bulletin*. **32**, 920-926 (2007).

39. J. Elliott: Novel approaches to multiscale modelling in materials science. *International Materials Reviews*. **56**, 207-225 (2011).

40. J. Jin, S. Shevlin, and Z. Guo: Multiscale simulation of onset plasticity during nanoindentation of Al (001) surface. *Acta Materialia*. **56**, 4358-4368 (2008).

41. R.E. Miller, L. Shilkrot, and W.A. Curtin: A coupled atomistics and discrete dislocation plasticity simulation of nanoindentation into single crystal thin films. *Acta Materialia*. **52**, 271-284 (2004).

42. F.-l. Zeng, Y. Sun, Y.-z. Liu, and Y. Zhou: Multiscale simulations of wedged nanoindentation on nickel. *Computational Materials Science*. **62**, 47-54 (2012).

43. P. Zhu, Y. Hu, F. Fang, and H. Wang: Multiscale simulations of nanoindentation and nanoscratch of single crystal copper. *Applied Surface Science*. **258**, 4624-4631 (2012).

44. O. Alizadeh, G.T. Eshlaghi, and S. Mohammadi: Nanoindentation simulation of coated aluminum thin film using quasicontinuum method. *Computational Materials Science*. **111**, 12-22 (2016).

45. F. Zeng, B. Zhao, and Y. Sun: Multiscale simulation of incipient plasticity and dislocation nucleation on nickel film during tilted flat-ended nanoindentation. *Acta Mechanica Solida Sinica*. **28**, 484-496 (2015).

46. Z. Fanlin and S. Yi: Quasicontinuum simulation of nanoindentation of nickel film. *Acta Mechanica Solida Sinica*. **19**, 283-288 (2006).

47. D. Shan, L. Wang, and L. Yuan: Effect of the  $\Sigma 5$  (310)/[001]  $\theta = 53.1^\circ$  grain boundary on the incipient yield of bicrystal copper: A quasicontinuum simulation and nanoindentation experiment. *Journal of Materials Research*. **28**, 766-773 (2013).

48. Z. Su, V. Tan, and T. Tay: Concurrent multiscale modeling of amorphous materials in 3D. *International Journal for Numerical Methods in Engineering*. **92**, 1081-1099 (2012).

49. A. Zhu, D. He, R. He, and C. Zou: Nanoindentation simulation on single crystal copper by quasi-continuum method. *Materials Science and Engineering: A*. **674**, 76-81 (2016).

50. T.-H. Fang, W.-J. Chang, D.-J. Yu, and C.-C. Huang: Microscopic properties of a nanocrystal aluminum thin film during nanoimprint using quasi-continuous method. *Thin Solid Films*. **612**, 237-242 (2016).

51. Z. Zhang and Y. Ni: Multiscale analysis of delay effect of dislocation nucleation with surface pit defect in nanoindentation. *Computational Materials Science*. **62**, 203-209 (2012).

52. H. Lu, Y. Ni, J. Mei, J. Li, and H. Wang: Anisotropic plastic deformation beneath surface step during nanoindentation of FCC Al by multiscale analysis. *Computational Materials Science*. **58**, 192-200 (2012).

53. J. Li, H. Lu, Y. Ni, and J. Mei: Quasicontinuum study the influence of misfit dislocation interactions on nanoindentation. *Computational Materials Science*. **50**, 3162-3170 (2011).

54. H. Lu, J. Li, and Y. Ni: Position effect of cylindrical indenter on nanoindentation into Cu thin film by multiscale analysis. *Computational Materials Science*. **50**, 2987-2992 (2011).

55. Y. Shao, X. Zhao, J. Li, and S. Wang: Multiscale simulations on the reversible plasticity of Al (001) surface under a nano-sized indenter. *Computational Materials Science*. **67**, 346-352 (2013).

56. W. Yu and S. Shen: Initial dislocation topologies of nanoindentation into copper (001) film with a nanocavity. *Engineering Fracture Mechanics*. **77**, 3329-3340 (2010).

57. J. Li, J. Mei, Y. Ni, H. Lu, and W. Jiang: Two-dimensional quasicontinuum analysis of the strengthening and weakening effect of Cu/Ag interface on nanoindentation. *Journal of Applied Physics*. **108**, 054309 (2010).

58. W. Yu and S. Shen: Effects of small indenter size and its position on incipient yield loading during nanoindentation. *Materials Science and Engineering: A.* **526**, 211-218 (2009).

59. W. Yu and S. Shen: Multiscale analysis of the effects of nanocavity on nanoindentation. *Computational Materials Science.* **46**, 425-430 (2009).

60. R.A. Iglesias and E.P. Leiva: Two-grain nanoindentation using the quasicontinuum method: Two-dimensional model approach. *Acta materialia.* **54**, 2655-2664 (2006).

61. X. Wei and J.W. Kysar: Experimental validation of multiscale modeling of indentation of suspended circular graphene membranes. *International Journal of Solids and Structures.* **49**, 3201-3209 (2012).

62. K.J. Van Vliet, J. Li, T. Zhu, S. Yip, and S. Suresh: Quantifying the early stages of plasticity through nanoscale experiments and simulations. *Physical Review B.* **67**, 104105 (2003).

63. Y. Zhong and T. Zhu: Simulating nanoindentation and predicting dislocation nucleation using interatomic potential finite element method. *Computer Methods in Applied Mechanics and Engineering.* **197**, 3174-3181 (2008).

64. S. Xu and X. Chen: Modeling dislocations and heat conduction in crystalline materials: atomistic/continuum coupling approaches. *International Materials Reviews.* 1-32 (2018).

65. B. Shiari, R.E. Miller, and W.A. Curtin: Coupled atomistic/discrete dislocation simulations of nanoindentation at finite temperature. *Journal of engineering materials and technology.* **127**, 358-368 (2005).

66. L. Xiong, G. Tucker, D.L. McDowell, and Y. Chen: Coarse-grained atomistic simulation of dislocations. *Journal of the Mechanics and Physics of Solids.* **59**, 160-177 (2011).

67. L. Xiong, Q. Deng, G. Tucker, D.L. McDowell, and Y. Chen: A concurrent scheme for passing dislocations from atomistic to continuum domains. *Acta Materialia.* **60**, 899-913 (2012).

68. S. Xu, L. Xiong, Q. Deng, and D.L. McDowell: Mesh refinement schemes for the concurrent atomistic-continuum method. *International Journal of Solids and Structures.* **90**, 144-152 (2016).

69. W.A. Curtin and R.E. Miller: A perspective on atomistic-continuum multiscale modeling. *Modelling and Simulation in Materials Science and Engineering.* **25**, 071004 (2017).

70. G. Ren, D. Zhang, and X.-G. Gong: Dynamical coupling atomistic and continuum simulations. *Communications in Computational Physics.* **10**, 1305-1314 (2011).

71. G. Ren, D. Zhang, and X. Gong: Dynamical multiscale simulation of nanoindentation. *Physics Letters A.* **375**, 953-956 (2011).

72. V. Iacobellis and K. Behdinan: Multiscale coupling using a finite element framework at finite temperature. *International Journal for Numerical Methods in Engineering*. **92**, 652-670 (2012).

73. V. Iacobellis and K. Behdinan: Bridging cell multiscale modeling of fatigue crack growth in fcc crystals. *International Journal for Numerical Methods in Engineering*. **104**, 1200-1216 (2015).

74. S.M.M. Zamani, V. Iacobellis, and K. Behdinan: Multiscale Modeling of the Nanodefects and Temperature Effect on the Mechanical Response of Sapphire. *Journal of the American Ceramic Society*. **99**, 2458-2466 (2016).

75. V. Iacobellis, A Bridging Cell Multiscale Methodology to Model the Structural Behaviour of Polymer Matrix Composites. 2016, University of Toronto.

76. B. Liu, H. Jiang, Y. Huang, S. Qu, M.-F. Yu, and K. Hwang: Atomic-scale finite element method in multiscale computation with applications to carbon nanotubes. *Physical Review B*. **72**, 035435 (2005).

77. B. Liu, Y. Huang, H. Jiang, S. Qu, and K. Hwang: The atomic-scale finite element method. *Computer methods in applied mechanics and engineering*. **193**, 1849-1864 (2004).

78. A.K. Subramaniyan and C. Sun: Engineering molecular mechanics: an efficient static high temperature molecular simulation technique. *Nanotechnology*. **19**, 285706 (2008).

79. V. Iacobellis and K. Behdinan: Bridging cell multiscale modeling of nanoindentation at finite temperature. *Transaction on Control and Mechanical Systems*. **2**, (2013).

80. Y. Chen, J. Zimmerman, A. Krivtsov, and D.L. McDowell: Assessment of atomistic coarse-graining methods. *International Journal of Engineering Science*. **49**, 1337-1349 (2011).

81. Y. Chen: Reformulation of microscopic balance equations for multiscale materials modeling. *The Journal of chemical physics*. **130**, 134706 (2009).

82. S. Xu, L. Xiong, Y. Chen, and D.L. McDowell: An analysis of key characteristics of the Frank-Read source process in FCC metals. *Journal of the Mechanics and Physics of Solids*. **96**, 460-476 (2016).

83. S. Xu, T.G. Payne, H. Chen, Y. Liu, L. Xiong, Y. Chen, and D.L. McDowell: PyCAC: The concurrent atomistic-continuum simulation environment. *Journal of Materials Research*. **33**, 857-871 (2018).

84. S. Xu, R. Che, L. Xiong, Y. Chen, and D.L. McDowell: A quasistatic implementation of the concurrent atomistic-continuum method for FCC crystals. *International Journal of Plasticity*. **72**, 91-126 (2015).

85. S. Yang, L. Xiong, Q. Deng, and Y. Chen: Concurrent atomistic and continuum simulation of strontium titanate. *Acta Materialia*. **61**, 89-102 (2013).

86. L. Shilkrot, R. Miller, and W. Curtin: Coupled atomistic and discrete dislocation plasticity. *Physical review letters*. **89**, 025501 (2002).

87. L. Shilkrot, R.E. Miller, and W.A. Curtin: Multiscale plasticity modeling: coupled atomistics and discrete dislocation mechanics. *Journal of the Mechanics and Physics of Solids*. **52**, 755-787 (2004).

88. J. Cho, T. Junge, J.-F. Molinari, and G. Anciaux: Toward a 3D coupled atomistic and discrete dislocation dynamics simulation: dislocation core structures and Peierls stresses with several character angles in FCC aluminum. *Advanced Modeling and Simulation in Engineering Sciences*. **2**, 12 (2015).

89. J. Cho, J.-F. Molinari, and G. Anciaux: Mobility law of dislocations with several character angles and temperatures in FCC aluminum. *International Journal of Plasticity*. **90**, 66-75 (2017).

90. F. Pavia and W. Curtin: Parallel algorithm for multiscale atomistic/continuum simulations using LAMMPS. *Modelling and Simulation in Materials Science and Engineering*. **23**, 055002 (2015).

91. G. Anciaux, T. Junge, M. Hodapp, J. Cho, J.-F. Molinari, and W. Curtin: The Coupled Atomistic/Discrete-Dislocation method in 3d part I: Concept and algorithms. *Journal of the Mechanics and Physics of Solids*. **118**, 152-171 (2018).

92. J. Cho, J.-F. Molinari, W.A. Curtin, and G. Anciaux: The coupled atomistic/discrete-dislocation method in 3d. Part III: Dynamics of hybrid dislocations. *Journal of the Mechanics and Physics of Solids*. **118**, 1-14 (2018).

93. M. Hodapp, G. Anciaux, J.-F. Molinari, and W. Curtin: Coupled atomistic/discrete dislocation method in 3D Part II: Validation of the method. *Journal of the Mechanics and Physics of Solids*. **119**, 1-19 (2018).

94. S. Qu, V. Shastry, W. Curtin, and R. Miller: A finite-temperature dynamic coupled atomistic/discrete dislocation method. *Modelling and Simulation in Materials Science and Engineering*. **13**, 1101 (2005).

95. B. Shiari and R.E. Miller: Multiscale modeling of crack initiation and propagation at the nanoscale. *Journal of the Mechanics and Physics of Solids*. **88**, 35-49 (2016).

96. B. Shiari, R.E. Miller, and D.D. Klug: Multiscale simulation of material removal processes at the nanoscale. *Journal of the Mechanics and Physics of Solids*. **55**, 2384-2405 (2007).

97. E. Lidorikis, M.E. Bachlechner, R.K. Kalia, A. Nakano, P. Vashishta, and G.Z. Voyatzis: Coupling length scales for multiscale atomistics-continuum simulations: atomistically induced stress distributions in Si/Si 3 N 4 nanopixels. *Physical review letters*. **87**, 086104 (2001).

98. J.Q. Broughton, F.F. Abraham, N. Bernstein, and E. Kaxiras: Concurrent coupling of length scales: methodology and application. *Physical review B*. **60**, 2391 (1999).

99. R.E. Rudd and J.Q. Broughton: Concurrent coupling of length scales in solid state systems. *physica status solidi (b)*. **217**, 251-291 (2000).

100. S. Ogata, E. Lidorikis, F. Shimojo, A. Nakano, P. Vashishta, and R.K. Kalia: Hybrid finite-element/molecular-dynamics/electronic-density-functional approach to materials simulations on parallel computers. *Computer Physics Communications*. **138**, 143-154 (2001).

101. C.-T. Wang, S.-R. Jian, J.S.-C. Jang, Y.-S. Lai, and P.-F. Yang: Multiscale simulation of nanoindentation on Ni (100) thin film. *Applied Surface Science*. **255**, 3240-3250 (2008).

102. E.B. Tadmor, M. Ortiz, and R. Phillips: Quasicontinuum analysis of defects in solids. *Philosophical magazine A*. **73**, 1529-1563 (1996).

103. E. Tadmor, F. Legoll, W. Kim, L. Dupuy, and R. Miller: Finite-temperature quasicontinuum. *Applied Mechanics Reviews*. **65**, 010803 (2013).

104. L.M. Dupuy, E.B. Tadmor, R.E. Miller, and R. Phillips: Finite-temperature quasicontinuum: Molecular dynamics without all the atoms. *Physical Review Letters*. **95**, 060202 (2005).

105. S. Li, W.K. Liu, A.J. Rosakis, T. Belytschko, and W. Hao: Mesh-free Galerkin simulations of dynamic shear band propagation and failure mode transition. *International Journal of solids and structures*. **39**, 1213-1240 (2002).

106. H. Li, T. Ng, J. Cheng, and K. Lam: Hermite–Cloud: a novel true meshless method. *Computational Mechanics*. **33**, 30-41 (2003).

107. W.K. Liu, S. Jun, and Y.F. Zhang: Reproducing kernel particle methods. *International journal for numerical methods in fluids*. **20**, 1081-1106 (1995).

108. A. Quarteroni and A. Valli, *Domain decomposition methods for partial differential equations*. Oxford University Press (1999).

109. T. Ng, V. Pandurangan, and H. Li: Multiscale modeling of nanoindentation in copper thin films via the concurrent coupling of the meshless Hermite–Cloud method with molecular dynamics. *Applied Surface Science*. **257**, 10613-10620 (2011).

110. V. Pandurangan, T. Ng, and H. Li: Nanoscratch Simulation on a Copper Thin Film Using a Novel Multiscale Model. *Journal of Nanomechanics and Micromechanics*. **4**, A4013008 (2013).

111. S. Xiao and W. Yang: A temperature - related homogenization technique and its implementation in the meshfree particle method for nanoscale simulations. *International journal for numerical methods in engineering*. **69**, 2099-2125 (2007).

112. T. Belytschko, Y.Y. Lu, and L. Gu: Element - free Galerkin methods. *International journal for numerical methods in engineering*. **37**, 229-256 (1994).

113. C. Dyka, P. Randles, and R. Ingel: Stress points for tension instability in SPH. *International Journal for Numerical Methods in Engineering*. **40**, 2325-2341 (1997).

114. S. Bardenhagen and E. Kober: The generalized interpolation material point method. *Computer Modeling in Engineering and Sciences*. **5**, 477-496 (2004).
115. J. Ma, Multiscale simulation using the generalized interpolation material point method, discrete dislocations and molecular dynamics. 2006, Oklahoma State University.
116. F.H. Harlow: The particle-in-cell computing method for fluid dynamics. *Methods in computational physics*. **3**, 319-343 (1964).
117. D. Sulusky, Z. Chen, and H.L. Schreyer: A particle method for history-dependent materials. *Computer methods in applied mechanics and engineering*. **118**, 179-196 (1994).
118. D. Sulusky, S.-J. Zhou, and H.L. Schreyer: Application of a particle-in-cell method to solid mechanics. *Computer physics communications*. **87**, 236-252 (1995).
119. A. Sadeghirad, R.M. Brannon, and J. Burghardt: A convected particle domain interpolation technique to extend applicability of the material point method for problems involving massive deformations. *International Journal for Numerical Methods in Engineering*. **86**, 1435-1456 (2011).
120. E. Van der Giessen and A. Needleman: Discrete dislocation plasticity: a simple planar model. *Modelling and Simulation in Materials Science and Engineering*. **3**, 689 (1995).
121. J. Ma, Y. Liu, H. Lu, and R. Komanduri: Multiscale simulation of nanoindentation using the generalized interpolation material point (GIMP) method, dislocation dynamics (DD) and molecular dynamics (MD). *Computer Modeling in Engineering and Sciences*. **16**, 41 (2006).
122. Q. Yang, E. Biyikli, and A.C. To: Multiresolution molecular mechanics: statics. *Computer methods in applied mechanics and engineering*. **258**, 26-38 (2013).
123. E. Biyikli, Q. Yang, and A.C. To: Multiresolution molecular mechanics: dynamics. *Computer methods in applied mechanics and engineering*. **274**, 42-55 (2014).
124. Q. Yang, E. Biyikli, and A.C. To: Multiresolution molecular mechanics: Convergence and error structure analysis. *Computer Methods in Applied Mechanics and Engineering*. **269**, 20-45 (2014).
125. Q. Yang and A.C. To: Multiresolution molecular mechanics: A unified and consistent framework for general finite element shape functions. *Computer Methods in Applied Mechanics and Engineering*. **283**, 384-418 (2015).
126. E. Biyikli and A.C. To: Multiresolution molecular mechanics: Adaptive analysis. *Computer Methods in Applied Mechanics and Engineering*. **305**, 682-702 (2016).
127. E. Biyikli and A.C. To: Multiresolution molecular mechanics: Implementation and efficiency. *Journal of Computational Physics*. **328**, 27-45 (2017).

128. Q. Yang and A.C. To: Multiresolution molecular mechanics: Surface effects in nanoscale materials. *Journal of Computational Physics*. **336**, 212-234 (2017).

129. P. Zhu, Y. Hu, and H. Wang: A hybrid model for multiscale simulations of nanoindentation. *Proceedings of the Institution of Mechanical Engineers, Part J: Journal of Engineering Tribology*. **225**, 845-853 (2011).

130. B. Luan, S. Hyun, J. Molinari, N. Bernstein, and M.O. Robbins: Multiscale modeling of two-dimensional contacts. *Physical Review E*. **74**, 046710 (2006).

131. B. Luan and M.O. Robbins: Hybrid atomistic/continuum study of contact and friction between rough solids. *Tribology letters*. **36**, 1-16 (2009).

132. E. McGee, R. Smith, and S. Kenny: Multiscale modelling of nanoindentation. *International journal of materials research*. **98**, 430-437 (2007).

133. A. Richter, C.-L. Chen, R. Smith, E. McGee, R. Thomson, and S. Kenny: Hot stage nanoindentation in multi-component Al–Ni–Si alloys: Experiment and simulation. *Materials Science and Engineering: A*. **494**, 367-379 (2008).

134. S.Z. Chavoshi, S. Xu, and S. Goel: Addressing the discrepancy of finding the equilibrium melting point of silicon using molecular dynamics simulations. *Proc. R. Soc. A*. **473**, 20170084 (2017).

135. S. Xu and S.Z. Chavoshi: Uniaxial deformation of nanotwinned nanotubes in body-centered cubic tungsten. *Current Applied Physics*. **18**, 114-121 (2018).

136. S. Xu, Y. Su, and S.Z. Chavoshi: Deformation of periodic nanovoid structures in Mg single crystals. *Materials Research Express*. (2018).

137. S.Z. Chavoshi, S.C. Gallo, H. Dong, and X. Luo: High temperature nanoscratching of single crystal silicon under reduced oxygen condition. *Materials Science and Engineering: A*. **684**, 385-393 (2017).

138. S. Xu and Y. Su: Dislocation nucleation from symmetric tilt grain boundaries in body-centered cubic vanadium. *Physics Letters A*. **382**, 1185-1189 (2018).

139. S. Xu, L. Xiong, Y. Chen, and D.L. McDowell: Comparing EAM potentials to model slip transfer of sequential mixed character dislocations across two symmetric tilt grain boundaries in Ni. *JOM*. **69**, 814-821 (2017).

140. S. Xu, J.K. Startt, T.G. Payne, C.S. Deo, and D.L. McDowell: Size-dependent plastic deformation of twinned nanopillars in body-centered cubic tungsten. *Journal of Applied Physics*. **121**, 175101 (2017).

141. C.A. Becker, F. Tavazza, Z.T. Trautt, and R.A.B. de Macedo: Considerations for choosing and using force fields and interatomic potentials in materials science and engineering. *Current Opinion in Solid State and Materials Science*. **17**, 277-283 (2013).

142. D. Brenner: The art and science of an analytic potential. *physica status solidi(b)*. **217**, 23-40 (2000).

143. J.A. Martinez, D.E. Yilmaz, T. Liang, S.B. Sinnott, and S.R. Phillpot: Fitting empirical potentials: Challenges and methodologies. *Current Opinion in Solid State and Materials Science*. **17**, 263-270 (2013).

144. J.D. Gale: Empirical potential derivation for ionic materials. *Philosophical Magazine B*. **73**, 3-19 (1996).

145. J.D. Gale: GULP: A computer program for the symmetry-adapted simulation of solids. *Journal of the Chemical Society, Faraday Transactions*. **93**, 629-637 (1997).

146. J.D. Gale and A.L. Rohl: The general utility lattice program (GULP). *Molecular Simulation*. **29**, 291-341 (2003).

147. B. Adams, M. Ebeida, M. Eldred, J. Jakeman, L. Swiler, W. Bohnhoff, and K. Dalbey, John Eddy, Kenneth Hu, Dena Vigil, Lara Baumann, and Patricia Hough.“Dakota, A Multilevel Parallel Object-Oriented Framework for Design Optimization, Parameter Estimation, Uncertainty Quantification, and Sensitivity Analysis”. 2013, Tech. rep., Sandia National Laboratories.

148. J.A. Martinez, A. Chernatynskiy, D.E. Yilmaz, T. Liang, S.B. Sinnott, and S.R. Phillpot: Potential Optimization Software for Materials (POSMat). *Computer Physics Communications*. **203**, 201-211 (2016).

149. M. Wen, S. Whalen, R. Elliott, and E. Tadmor: Interpolation effects in tabulated interatomic potentials. *Modelling and Simulation in Materials Science and Engineering*. **23**, 074008 (2015).

150. M.S. Daw and M.I. Baskes: Embedded-atom method: Derivation and application to impurities, surfaces, and other defects in metals. *Physical Review B*. **29**, 6443-6453 (1984).

151. J.E. Angelo, N.R. Moody, and M.I. Baskes: Trapping of hydrogen to lattice defects in nickel. *Modelling and Simulation in Materials Science and Engineering*. **3**, 289 (1995).

152. D.W. Brenner: Empirical potential for hydrocarbons for use in simulating the chemical vapor deposition of diamond films. *Physical Review B*. **42**, 9458-9471 (1990).

153. D.W. Brenner: Erratum: Empirical potential for hydrocarbons for use in simulating the chemical vapor deposition of diamond films. *Physical Review B*. **46**, 1948 (1992).

154. G. Gochola, S.P. Russo, and I.K. Snook: On fitting a gold embedded atom method potential using the force matching method. *The Journal of chemical physics*. **123**, 204719 (2005).

155. S. Roy and D. Mordehai: Annihilation of edge dislocation loops via climb during nanoindentation. *Acta Materialia*. (2017).

156. S.Z. Chavoshi and S. Xu: Twinning effects in the single/nanocrystalline cubic silicon carbide subjected to nanoindentation loading. Submitted. (2018).

157. S. Amaya-Roncancio, D. Arias-Mateus, M. Gomez-Hermida, J. Riano-Rojas, and E. Restrepo-Parra: Molecular dynamics simulations of the temperature effect in the hardness on Cr and CrN films. *Applied Surface Science*. **258**, 4473-4477 (2012).

158. R. Komanduri, N. Chandrasekaran, and L. Raff: Molecular dynamics (MD) simulation of uniaxial tension of some single-crystal cubic metals at nanolevel. *International Journal of Mechanical Sciences*. **43**, 2237-2260 (2001).

159. K. Xiong, H. Lu, and J. Gu: Atomistic simulations of the nanoindentation-induced incipient plasticity in Ni<sub>3</sub>Al crystal. *Computational Materials Science*. **115**, 214-226 (2016).

160. J. Du, C. Wang, and T. Yu: Construction and application of multi-element EAM potential (Ni - Al - Re) in  $\gamma/\gamma'$  Ni-based single crystal superalloys. *Modelling and Simulation in Materials Science and Engineering*. **21**, 015007 (2013).

161. H. Liu, K. Chen, Y. Gong, G. An, and Z. Hu: Properties of the liquid-vapour interface of fcc metals calculated using the tight-binding potential. *Philosophical Magazine A*. **75**, 1067-1074 (1997).

162. K. Maekawa and A. Itoh: Friction and tool wear in nano-scale machining—a molecular dynamics approach. *Wear*. **188**, 115-122 (1995).

163. T.-H. Fang, C.-I. Weng, and J.-G. Chang: Molecular dynamics analysis of temperature effects on nanoindentation measurement. *Materials Science and Engineering: A*. **357**, 7-12 (2003).

164. C.-L. Liu, T.-H. Fang, and J.-F. Lin: Atomistic simulations of hard and soft films under nanoindentation. *Materials Science and Engineering: A*. **452**, 135-141 (2007).

165. J.-Y. Hsieh, S.-P. Ju, S.-H. Li, and C.-C. Hwang: Temperature dependence in nanoindentation of a metal substrate by a diamondlike tip. *Physical Review B*. **70**, 195424-195433 (2004).

166. D. Liu, C. Tsai, and S. Lyu: Determination of temperature-dependent elasto-plastic properties of thin-film by MD nanoindentation simulations and an inverse GA/FEM computational scheme. *Computers, Materials & Continua (CMC)*. **11**, 147 (2009).

167. F. Cleri and V. Rosato: Tight-binding potentials for transition metals and alloys. *Physical Review B*. **48**, 22 (1993).

168. P. Vashishta, R.K. Kalia, A. Nakano, and J.P. Rino: Interaction potential for silicon carbide: a molecular dynamics study of elastic constants and vibrational density of states for crystalline and amorphous silicon carbide. *Journal of applied physics*. **101**, 103515-103528 (2007).

169. T.-H. Fang and J.-H. Wu: Molecular dynamics simulations on nanoindentation mechanisms of multilayered films. *Computational Materials Science*. **43**, 785-790 (2008).

170. N. Papanicolaou, H. Chamati, G. Evangelakis, and D. Papaconstantopoulos: Second-moment interatomic potential for Al, Ni and Ni-Al alloys, and molecular dynamics application. *Computational materials science*. **27**, 191-198 (2003).

171. C.-D. Wu, T.-H. Fang, and C.-Y. Chan: A molecular dynamics simulation of the mechanical characteristics of a C 60-filled carbon nanotube under nanoindentation using various carbon nanotube tips. *Carbon*. **49**, 2053-2061 (2011).

172. J. Tersoff: Modeling solid-state chemistry: Interatomic potentials for multicomponent systems. *Physical Review B*. **39**, 5566-5568 (1989).

173. J. Tersoff: Erratum: Modeling solid-state chemistry: Interatomic potentials for multicomponent systems. *Physical Review B*. **41**, 3248-3248 (1990).

174. J. Tersoff: Empirical interatomic potential for silicon with improved elastic properties. *Physical Review B*. **38**, 9902-9905 (1988).

175. J. Tersoff: New empirical approach for the structure and energy of covalent systems. *Physical Review B*. **37**, 6991-7000 (1988).

176. C. Huang, X. Peng, T. Fu, Y. Zhao, C. Feng, Z. Lin, and Q. Li: Nanoindentation of ultra-hard cBN films: A molecular dynamics study. *Applied Surface Science*. **392**, 215-224 (2017).

177. J.-W. Jiang, H.S. Park, and T. Rabczuk: Molecular dynamics simulations of single-layer molybdenum disulphide (MoS<sub>2</sub>): Stillinger-Weber parametrization, mechanical properties, and thermal conductivity. *Journal of Applied Physics*. **114**, 064307 (2013).

178. T. Liang, S.R. Phillpot, and S.B. Sinnott: Parametrization of a reactive many-body potential for Mo-S systems. *Physical Review B*. **79**, 245110 (2009).

179. J. Zhao, J.-W. Jiang, and T. Rabczuk: Temperature-dependent mechanical properties of single-layer molybdenum disulphide: Molecular dynamics nanoindentation simulations. *Applied Physics Letters*. **103**, 231913 (2013).

180. W. Wang, L. Li, C. Yang, R. Soler-Crespo, Z. Meng, M. Li, X. Zhang, S. Keten, and H. Espinosa: Plasticity Resulted from Phase Transformation for Monolayer Molybdenum Disulfide Film during Nanoindentation Simulations. *Nanotechnology*. (2017).

181. F. Delogu: A molecular dynamics study on the role of localised lattice distortions in the formation of Ni-Zr metallic glasses. *Materials Science and Engineering: A*. **359**, 52-61 (2003).

182. C.-H. Wang, K.-C. Chao, T.-H. Fang, I. Stachiv, and S.-F. Hsieh: Investigations of the mechanical properties of nanoimprinted amorphous Ni-Zr alloys utilizing the molecular dynamics simulation. *Journal of Alloys and Compounds*. **659**, 224-231 (2016).

183. A. Argon: Plastic deformation in metallic glasses. *Acta metallurgica*. **27**, 47-58 (1979).

184. A. Argon and L.T. Shi: Development of visco-plastic deformation in metallic glasses. *Acta Metallurgica*. **31**, 499-507 (1983).

185. R. Zallen, *The physics of amorphous solids*. John Wiley & Sons (2008).

186. C. Qiu, P. Zhu, F. Fang, D. Yuan, and X. Shen: Study of nanoindentation behavior of amorphous alloy using molecular dynamics. *Applied Surface Science*. **305**, 101-110 (2014).

187. M. Mendelev, M. Kramer, R. Ott, D. Sordelet, D. Yagodin, and P. Popel: Development of suitable interatomic potentials for simulation of liquid and amorphous Cu-Zr alloys. *Philosophical Magazine*. **89**, 967-987 (2009).

188. C.-H. Wang, T.-H. Fang, P.-C. Cheng, C.-C. Chiang, and K.-C. Chao: Simulation and experimental analysis of nanoindentation and mechanical properties of amorphous NiAl alloys. *Journal of molecular modeling*. **21**, 161 (2015).

189. W.H. Wang: The elastic properties, elastic models and elastic perspectives of metallic glasses. *Progress in Materials Science*. **57**, 487-656 (2012).

190. Y. Mishin, M. Mehl, D. Papaconstantopoulos, A. Voter, and J. Kress: Structural stability and lattice defects in copper: Ab initio, tight-binding, and embedded-atom calculations. *Physical Review B*. **63**, 224106 (2001).

191. T. Inamura, N. Takezawa, and N. Taniguchi: Atomic-scale cutting in a computer using crystal models of copper and diamond. *CIRP Annals-Manufacturing Technology*. **41**, 121-124 (1992).

192. V. Pandurangan, H. Li, and T. Ng: A concurrent multiscale method based on the alternating Schwarz scheme for coupling atomic and continuum scales with first-order compatibility. *Computational Mechanics*. **47**, 1-16 (2011).

193. H. Pen, Y. Liang, X. Luo, Q. Bai, S. Goel, and J. Ritchie: Multiscale simulation of nanometric cutting of single crystal copper and its experimental validation. *Computational Materials Science*. **50**, 3431-3441 (2011).

194. X. Sun, S. Chen, K. Cheng, D. Huo, and W. Chu: Multiscale simulation on nanometric cutting of single crystal copper. *Proceedings of the Institution of Mechanical Engineers, Part B: Journal of Engineering Manufacture*. **220**, 1217-1222 (2006).

195. X. Sun and K. Cheng: Multi-scale simulation of the nano-metric cutting process. *The International Journal of Advanced Manufacturing Technology*. **47**, 891-901 (2010).

196. L. Zhang, H. Zhao, W. Guo, Z. Ma, and X. Wang: Quasicontinuum analysis of the effect of tool geometry on nanometric cutting of single crystal copper. *Optik-International Journal for Light and Electron Optics*. **125**, 682-687 (2014).

197. C. Fang, X. Meng, Y. Xie, and B. Zhao: Quasicontinuum investigation of the feedback effects on friction behavior of an abrasive particle over a single crystal aluminum substrate. *Tribology International*. **98**, 48-58 (2016).

198. J.-S. Wang, X.-D. Zhang, X.-W. Chen, M. Lai, and F.-F. Xu: Effect of crystal orientations on nanocutting based on quasicontinuum multiscale method. *International Journal of Nanomanufacturing*. **10**, 371-389 (2014).

199. S.Z. Chavoshi, S. Goel, and X. Luo: Molecular dynamics simulation investigation on the plastic flow behaviour of silicon during nanometric cutting. *Modelling and Simulation in Materials Science and Engineering*. **24**, 015002 (2015).

200. S.Z. Chavoshi and X. Luo: Atomic-scale characterization of occurring phenomena during hot nanometric cutting of single crystal 3C-SiC. *RSC Advances*. **6**, 71409-71424 (2016).

201. S.Z. Chavoshi and X. Luo: An atomistic simulation investigation on chip related phenomena in nanometric cutting of single crystal silicon at elevated temperatures. *Computational Materials Science*. **113**, 1-10 (2016).

202. S.Z. Chavoshi, S. Goel, and X. Luo: Influence of temperature on the anisotropic cutting behaviour of single crystal silicon: A molecular dynamics simulation investigation. *Journal of Manufacturing Processes*. **23**, 201-210 (2016).

203. C.-D. Wu, T.-H. Fang, and J.-K. Su: Nanometric mechanical cutting of metallic glass investigated using atomistic simulation. *Applied Surface Science*. **396**, 319-326 (2017).

204. F.H. Stillinger and T.A. Weber: Computer simulation of local order in condensed phases of silicon. *Physical Review B*. **31**, 5262-5271 (1985).

205. P. Erhart and K. Albe: Analytical potential for atomistic simulations of silicon, carbon, and silicon carbide. *Physical Review B*. **71**, 035211-035225 (2005).

206. S.Z. Chavoshi and X. Luo: Molecular dynamics simulation study of deformation mechanisms in 3C-SiC during nanometric cutting at elevated temperatures. *Materials Science and Engineering: A*. **654**, 400-417 (2016).

207. G.P. Pun and Y. Mishin: Optimized interatomic potential for silicon and its application to thermal stability of silicene. *Physical Review B*. **95**, 224103 (2017).

208. S. Coleman, D. Spearot, and L. Capolungo: Virtual diffraction analysis of Ni [0 1 0] symmetric tilt grain boundaries. *Modelling and Simulation in Materials Science and Engineering*. **21**, 055020-055036 (2013).

209. S.Z. Chavoshi, S. Xu, and X. Luo: Dislocation-mediated plasticity in silicon during nanometric cutting: A molecular dynamics simulation study. *Materials Science in Semiconductor Processing*. **51**, 60-70 (2016).

210. T. Zykova-Timan, D. Ceresoli, and E. Tosatti: Peak effect versus skating in high-temperature nanofriction. *Nature materials*. **6**, 230-234 (2007).

211. F.G. Fumi and M. Tosi: Ionic sizes and born repulsive parameters in the NaCl-type alkali halides—I: The Huggins-Mayer and Pauling forms. *Journal of Physics and Chemistry of Solids*. **25**, 31-43 (1964).

212. M. Tosi and F. Fumi: Ionic sizes and born repulsive parameters in the NaCl-type alkali halides—II: The generalized Huggins-Mayer form. *Journal of Physics and Chemistry of Solids*. **25**, 45-52 (1964).

213. E. Meyer and E. Gnecco: Nanofriction: Skating on hot surfaces. *Nature materials*. **6**, 180-181 (2007).

214. R. Crawford, J. Taylor, and D. Keefer: Solid ring armature experiments in a transaugmented railgun. *IEEE transactions on magnetics*. **31**, 138-143 (1995).

215. E. Drobyshevski, E. Kolesnikova, and V. Yuferev: Calculating the liquid film effect on solid armature rail-gun launching. *IEEE transactions on magnetics*. **35**, 53-58 (1999).

216. B. He, G. Ghosh, Y.-W. Chung, and Q. Wang: Effect of Melting and Microstructure on the microscale friction of silver–bismuth alloys. *Tribology letters*. **38**, 275-282 (2010).

217. K. Mizushima, S. Yip, and E. Kaxiras: Ideal crystal stability and pressure-induced phase transition in silicon. *Physical Review B*. **50**, 14952 (1994).

218. A.F. Voter: Parallel replica method for dynamics of infrequent events. *Physical Review B*. **57**, R13985 (1998).

219. M.R. So/rensen and A.F. Voter: Temperature-accelerated dynamics for simulation of infrequent events. *The Journal of Chemical Physics*. **112**, 9599-9606 (2000).

220. F. Roters, P. Eisenlohr, T.R. Bieler, and D. Raabe, *Crystal plasticity finite element methods: in materials science and engineering*. John Wiley & Sons (2011).

221. F. Roters, P. Eisenlohr, L. Hantcherli, D.D. Tjahjanto, T.R. Bieler, and D. Raabe: Overview of constitutive laws, kinematics, homogenization and multiscale methods in crystal plasticity finite-element modeling: Theory, experiments, applications. *Acta Materialia*. **58**, 1152-1211 (2010).

222. D. Faghihi and G.Z. Voyiadjis: Determination of nanoindentation size effects and variable material intrinsic length scale for body-centered cubic metals. *Mechanics of Materials*. **44**, 189-211 (2012).

223. Q. Yang, E. Biyikli, P. Zhang, R. Tian, and A.C. To: Atom collocation method. *Computer methods in applied mechanics and engineering*. **237**, 67-77 (2012).

224. R. Gracie and T. Belytschko: Concurrently coupled atomistic and XFEM models for dislocations and cracks. *International Journal for Numerical Methods in Engineering*. **78**, 354-378 (2009).

225. R. Gracie and T. Belytschko: An adaptive concurrent multiscale method for the dynamic simulation of dislocations. *International Journal for Numerical Methods in Engineering*. **86**, 575-597 (2011).

226. R. Agrawal and H. Espinosa: Multiscale experiments: state of the art and remaining challenges. *Journal of Engineering Materials and Technology*. **131**, 041208 (2009).

